Physics Letters B 774 (2017) 279–307

Contents lists available at ScienceDirect

Physics Letters B

www.elsevier.com/locate/physletb

Search for black holes and other new phenomena in high-multiplicity final states in proton–proton collisions at $\sqrt{s} = 13\,\text{TeV}$

The CMS Collaboration *

CERN, Switzerland

ARTICLE INFO

Article history:
Received 3 May 2017
Received in revised form 15 August 2017
Accepted 11 September 2017
Available online 22 September 2017
Editor: M. Doser

Keywords:
CMS
Physics
Black holes

ABSTRACT

A search for new physics in energetic, high-multiplicity final states has been performed using proton–proton collision data collected with the CMS detector at a center-of-mass energy of 13 TeV and corresponding to an integrated luminosity of $2.3\,\text{fb}^{-1}$. The standard model background, dominated by multijet production, is determined exclusively from control regions in data. No statistically significant excess of events is observed. Model-independent limits on the product of the cross section and the acceptance of a new physics signal in these final states are set and further interpreted in terms of limits on the production of black holes. Semiclassical black holes and string balls with masses as high as 9.5 TeV, and quantum black holes with masses as high as 9.0 TeV are excluded by this search in the context of models with extra dimensions, thus significantly extending limits set at a center-of-mass energy of 8 TeV with the LHC Run 1 data.

© 2017 The Author(s). Published by Elsevier B.V. This is an open access article under the CC BY license (http://creativecommons.org/licenses/by/4.0/). Funded by SCOAP[3].

1. Introduction

The standard model (SM) [1–3] of particle physics is a remarkably successful theory. However, several outstanding problems remain. One of these is the "hierarchy problem" [4], i.e., the vast separation between the electroweak energy scale and the scale at which gravity becomes strong. The latter, referred to as the "Planck scale" (M_{Pl}), is some 17 orders of magnitude greater than the former. There are various theoretical extensions of the SM that address the hierarchy problem, such as supersymmetry (SUSY) and models with extra dimensions.

In many of these models, high-multiplicity, energetic final states naturally occur. Strong single or pair production of various new physics signals result in multijet final states, often accompanied by energetic leptons and/or invisible particles resulting in transverse momentum (p_{T}) imbalance in the event. Examples include a large variety of SUSY signals, both with R-parity [5] conservation [6] and violation [7], and signals associated with technicolor models [8], axigluons [9], colorons [10–13], and various models with low-scale gravity.

In this Letter, we describe a model-independent search for new physics in high-multiplicity final states, and explicitly test the predictions of two possible solutions to the hierarchy problem. One of these solutions invokes a model with n large extra dimensions, colloquially known as the "ADD model", named after its proponents, Arkani-Hamed, Dimopoulos, and Dvali [14–16]. The other solution is based on the Randall–Sundrum model [17,18], called the "RS1 model". In this model a single, compact extra spatial dimension is warped, and the SM particles are localized on a TeV-scale brane, while gravity originates on the second, Planck brane, separated from the TeV brane in the extra dimension.

In the ADD model, the fundamental multidimensional Planck scale (M_{D}) is related to the "apparent" 3-dimensional Planck scale M_{Pl} as:

$$M_{\text{D}} = \frac{1}{r}\left(\frac{rM_{\text{Pl}}}{\sqrt{8\pi}}\right)^{\frac{2}{n+2}}, \tag{1}$$

where r is the compactification radius or the characteristic size of extra dimensions.

In the RS1 model, the analog of the ADD scale M_{D} is defined as a function of the exponential warp factor k and the compactification radius r:

$$M_{\text{D}} = \frac{M_{\text{Pl}}}{\sqrt{8\pi}} e^{-\pi kr}. \tag{2}$$

In both models, M_{D} can be of order 1 TeV, thus eliminating the hierarchy of scales and alleviating the hierarchy problem.

At high-energy hadron colliders, such as the CERN LHC, if the collision energy exceeds M_{D}, both the ADD and RS1 models allow for the formation of microscopic black holes (BHs) [19–23].

* *E-mail address:* cms-publication-committee-chair@cern.ch.

https://doi.org/10.1016/j.physletb.2017.09.053
0370-2693/© 2017 The Author(s). Published by Elsevier B.V. This is an open access article under the CC BY license (http://creativecommons.org/licenses/by/4.0/). Funded by SCOAP[3].

In the simplest scenario, microscopic BHs are produced when the distance of closest approach between two colliding particles is less than the Schwarzschild radius R_S, which for a BH in a $(3+n)$-dimensional space is given by [24]:

$$R_S = \frac{1}{\sqrt{\pi} M_D}\left[\frac{M_{BH}}{M_D}\left(\frac{8\Gamma(\frac{n+3}{2})}{n+2}\right)\right]^{\frac{1}{n+1}}, \quad (3)$$

where M_{BH} is the mass of the BH. The parton-level production cross section of such processes is expected to be simply πR_S^2 [19,20]. In more complicated scenarios with energy loss during the formation of the BH horizon, the production cross section could significantly depart from this simple geometrical formula. Since the production of BHs is a threshold phenomenon, we assume a minimum mass threshold $M_{BH}^{min} \geq M_D$.

In the semiclassical case, corresponding to $M_{BH} \gg M_D$, BHs evaporate rapidly via Hawking radiation [25], with a lifetime of order 10^{-27} seconds. As gravity couples universally to the energy-momentum tensor and does not distinguish between various particle species, microscopic BHs decay democratically into all SM degrees of freedom, i.e., all SM particle species with all possible values of quantum numbers, such as spin, color, and charge. The final state is therefore populated by a variety of energetic particles, such as hadrons (jets), leptons, photons, and neutrinos. Due to the large number of color degrees of freedom, about 75% of the particles produced are expected to be quarks and gluons. The final state may contain significant transverse momentum imbalance from the presence of neutrinos, which constitute about 5% of the decay products. Other processes, such as the decay of W and Z bosons, or of heavy-flavor quarks, and the possible emission of gravitons or the formation of a noninteracting stable BH remnant, contribute to the transverse momentum imbalance as well.

The semiclassical approximation breaks down when the mass of the BH approaches M_D and the BH becomes a quantum object or a quantum black hole (QBH). These objects do not obey the usual BH thermodynamics and hence decay much more rapidly than their semiclassical counterparts. Their decays are characterized by the presence of only a few particles, e.g., a pair of jets [26–28]. These QBHs could also decay into lepton flavor violating final states, as preserving baryon number or lepton numbers separately is typically not a requirement of the decay process [26,27].

In addition to semiclassical BHs and QBHs, one could also explore stringy precursors of BHs, called "string balls" (SBs) [29]. Such objects, which arise in string theory, are highly excited, long, folded strings that form below the BH production threshold. Like semiclassical BHs, SBs evaporate thermally, but at a constant Hagedorn temperature [30] independent of the SB mass, and also produce a large number of energetic particles in the final state, with the composition similar to that for a semiclassical BH. String balls undergo a phase transition into ordinary semiclassical BHs when their mass reaches M_S/g_S^2 [29], where M_S and g_S are the string scale and the string coupling constant, respectively. For an SB mass between M_S/g_S and the BH transition, M_S/g_S^2, the parton-level cross section saturates at $\sigma \sim 1/M_S^2$, while for lighter SBs, it grows as $\sigma \sim g_S^2 M_{SB}^2/M_S^4$ [29].

While our choice of final states is inspired by the production of microscopic BHs, in this Letter we focus on a generic search (Section 8) that can be used to probe a large class of new-physics models. Consequently, our emphasis is on the exploration of a multiparticle final state with a model-independent search.

During Run 1 of the LHC, a number of searches for semiclassical and quantum BHs were performed at a center-of-mass energy of 8 TeV. A review of these results can be found in Ref. [31]. The limits on the minimum BH mass set by these searches lie in the 6 TeV range. With the increased LHC center-of-mass energy of 13 TeV, the BH phase space can be probed much more extensively, as was demonstrated in the recent ATLAS publications [32–34], which set BH mass limits reaching 9 TeV.

2. Analysis strategy

The most challenging aspect of the analysis presented in this Letter is accurately describing the QCD multijet background, since the BH signal leads to a broad excess in the S_T spectrum, rather than a narrow peak. Here, S_T is defined as the scalar sum of the transverse energies of jets, leptons, photons, as well as the missing transverse energy (E_T^{miss}, defined as the magnitude of the transverse momentum imbalance in an event, as detailed in Section 4):

$$S_T = \left(\sum_{i=1}^{N} E_{T,i}\right) + E_T^{miss}, \quad (4)$$

where N is the total number of final-state objects (excluding the E_T^{miss}), or the object multiplicity. For the QCD background, the final-state objects are almost exclusively jets and the E_T^{miss} is expected to be small, so the S_T variable is reduced to a scalar sum of the transverse momenta of the jets. The signal region for this search typically lies in the high-multiplicity regime where the QCD multijet background is dominated by higher-order effects. These effects have not been calculated for high-multiplicity final states, and therefore an accurate simulation of the QCD multijet background, pertinent to our signal region, does not yet exist.

This significant hurdle is mitigated by predicting the QCD multijet background directly from data using a new technique developed in Run 1 of the LHC [35–37]. Studies performed with simulated QCD multijet events and with data at low object multiplicities show that the shape of the S_T distribution above its turn-on threshold is approximately independent of the multiplicity of the final state. This observation is consistent with the development of the parton shower via nearly collinear emission, which approximately conserves the S_T value, up to the effects of additional jets falling below the kinematic threshold. For this reason one can predict the S_T spectrum of a multijet final state using samples of dijet or trijet events. This feature provides a powerful tool to predict the shape of the S_T spectrum at higher multiplicity using a low-multiplicity control region. The method has found wide applicability in various CMS searches, such as a search for stealth SUSY [38] and a search for multijet resonances [39]. An earlier CMS analysis [35] also considered other kinematic variables, such as the invariant mass or transverse invariant mass of the event. However, the multiplicity invariance is not exhibited by these variable to the degree shown by the S_T variable.

In this Letter we follow closely the methodology of Refs. [35–37] geared toward a multiparticle final state, dominated by QCD multijets in the case of semiclassical BHs, and toward a dijet final state for the QBHs. The variable S_T is the single discriminating variable used in the analysis, chosen for its robustness against variations in the BH evaporation model and its lack of sensitivity to the relative abundance of various particles produced. This variable encompasses the total transverse energy in an event and is therefore useful in discriminating between the signal and the background. There is a minimum transverse energy (E_T) threshold of 50 GeV [35] that each of the objects (including the E_T^{miss}) has to satisfy to be counted toward the definition of S_T. The exact choice of the E_T threshold is not particularly important; the 50 GeV threshold is chosen as it makes the analysis insensitive to additional interactions in the same or adjacent bunch crossings (pileup) and moderates the effect of initial-state radiation, which generally spoils the S_T invariance.

The S_T distributions are produced in a number of inclusive object multiplicity bins ($N \geq N^{\min}$). The background is estimated exclusively from collision data via the appropriately chosen control regions. This approach does not rely on the Monte Carlo (MC) description of the backgrounds. In addition, this method has the advantage of being more sensitive and less model dependent than exclusive searches in specific final states, e.g., the lepton + jets final state [40,41]. The ATLAS Collaboration has recently adopted a similar inclusive search strategy based on the 2012 $\sqrt{s} = 8$ TeV [42] and the 2015 $\sqrt{s} = 13$ TeV data [33].

3. The CMS detector

The central feature of the CMS apparatus is a superconducting solenoid of 6 m internal diameter, providing a magnetic field of 3.8 T. Within the solenoid volume are a silicon pixel and strip tracker, a lead tungstate crystal electromagnetic calorimeter (ECAL), and a brass and scintillator hadron calorimeter (HCAL), each composed of a barrel and two endcap sections. Forward calorimeters extend the pseudorapidity coverage provided by the barrel and endcap detectors up to $|\eta| < 5$. Muons are measured in gas-ionization detectors embedded in the steel flux-return yoke outside the solenoid.

The silicon tracker measures charged particles within the pseudorapidity range $|\eta| < 2.5$. It consists of 1440 silicon pixel and 15 148 silicon strip detector modules. For nonisolated particles of $1 < p_T < 10$ GeV and $|\eta| < 1.4$, the track resolutions are typically 1.5% in p_T and 25–90 (45–150) μm in the transverse (longitudinal) impact parameter [43].

In the region $|\eta| < 1.74$, the HCAL cells have widths of 0.087 in pseudorapidity and 0.087 radians in azimuth (ϕ). In the η–ϕ plane, and for $|\eta| < 1.48$, the HCAL cells map on to 5×5 arrays of ECAL crystals to form calorimeter towers projecting radially outwards from close to the nominal interaction point. For $|\eta| > 1.74$, the coverage of the towers increases progressively to a maximum of 0.174 in $\Delta\eta$ and $\Delta\phi$. Within each tower, the energy deposits in ECAL and HCAL cells are summed to define the calorimeter tower energies, subsequently used to provide the energies and directions of hadronic jets.

The first level of the CMS trigger system [44], composed of custom hardware processors, combines information from the calorimeters and muon detectors to select the most interesting events in a fixed time interval of 3.2 μs. The high-level trigger (HLT) processor farm further decreases the event rate from around 100 kHz to less than 1 kHz, before data storage.

A detailed description of the CMS detector, together with a definition of the coordinate system used and the relevant kinematic variables, can be found in Ref. [45].

4. Event reconstruction

The analysis is based on proton–proton collision data corresponding to an integrated luminosity of 2.3 fb^{-1}, collected with the CMS detector in 2015. The trigger chosen for the analysis is based on the total transverse energy of jets in an event. At the HLT, events are selected if they passed an 800 GeV threshold on the scalar sum of the transverse momenta of all hadronic jets, which are reconstructed with the particle-flow (PF) algorithm [46], as described below. The trigger is nearly 100% efficient for S_T above 1 TeV.

In the subsequent analysis, we select events with at least one reconstructed vertex [43] within 24 (2) cm of the nominal interaction point measured parallel (perpendicular) to the LHC beamline. The vertex with the highest sum of the transverse momenta squared of the associated tracks is chosen as the hard-scattering vertex.

The reconstruction of physics objects in the event is based on the PF algorithm that identifies each single particle in an event (photon, electron, muon, charged hadron, neutral hadron) using an optimized combination of all subdetector information. The energy of photons is directly obtained from the ECAL measurement, corrected for zero-suppression effects [47]. The energy of electrons is determined from a combination of the track momentum at the main interaction vertex, the corresponding ECAL cluster energy, and the energy sum of all bremsstrahlung photons attached to the track. The energy of muons is obtained from the corresponding track momentum. The energy of charged hadrons is determined from a combination of the track momentum and the corresponding ECAL and HCAL energy, corrected for zero-suppression effects and for the response function of the calorimeters to hadronic showers. The energy of neutral hadrons is obtained from the corresponding corrected ECAL and HCAL energy. Finally, the E_T^{miss} is defined as the absolute value of the vectorial p_T sum of all the PF candidates reconstructed in an event [48].

For each event, hadronic jets are clustered from the PF candidates using the anti-k_T algorithm [49] with a distance parameter of 0.4, as implemented in the FastJet package [50]. The jet momentum is determined as the vectorial sum of the momenta of all its constituents, and is found to be within 5 to 10% of the true (particle-level) momentum over the whole p_T spectrum and the detector acceptance. Jet energy corrections are derived from simulation and in situ measurements of the energy balance in dijet, multijet, γ + jet, and leptonic Z + jet events [51,52]. The contribution of charged hadrons that do not originate from the hard-scattering vertex ("pileup"), but are clustered during the reconstruction of a jet, is subtracted. Corrections based on the jet area [53] are applied to remove the energy contribution of neutral hadrons from pileup interactions. The jet energy resolution (JER) is approximately 8% at 100 GeV and 4% at 1 TeV [51,52]. The minimum threshold on the corrected E_T of the jets used in the analysis is 50 GeV, and jets are accepted in the full pseudorapidity range of the CMS calorimeters ($|\eta| < 5$). To reduce contamination from poorly reconstructed muons, the fraction of the jet momentum carried by a muon is required to be less than 80%. Also, to suppress jets due to rare, spurious anomalous calorimeter signals, jets must contain at least two particles, one of which is a charged hadron, and the jet energy fraction carried by neutral PF candidates (neutral hadrons and photons) should be less than 90%. These criteria have an efficiency greater than 99% per jet.

Details of muon reconstruction can be found in Ref. [54]. Muon candidates are required to satisfy a minimum p_T threshold of 50 GeV and to be within $|\eta| < 2.4$. The transverse impact parameter and the longitudinal distance of the track associated with the muon with respect to the primary vertex is required to be less than 2 and 5 mm, respectively, to reduce contamination from cosmic muons. The muon candidate is required to have at least one energy deposit in the pixel tracker and at least six deposits in the silicon strip tracker. The global track fit to the tracker trajectory and to at least two muon detector segments must have a χ^2 per degree of freedom of less than 10.

Details of electron reconstruction can be found in Ref. [55]. Electron candidates are required to have $E_T > 50$ GeV, $|\eta| < 2.5$, excluding the $1.44 < |\eta| < 1.57$ transition region between the ECAL barrel and endcap detectors where the reconstruction is suboptimal, and to pass standard identification criteria, corresponding to a working point with an average efficiency of 80% per electron.

Both muons and electrons are required to be isolated from other energy deposits in the tracker and the calorimeters. The relative isolation $\mathcal{I}$ is defined as the ratio of the sum of transverse

Table 1
Generator settings for various semiclassical BH model points probed in this analysis. These parameters are defined in Refs. [56] and [57] for the BlackMax and charybdis 2 generators, respectively. The generator settings not specified are kept at their default values.

BlackMax

Model	Choose_a_case	Mass_loss_factor	Momentum_loss_factor	turn_on_graviton
B1	tensionless_nonrotating	0	0	FALSE
B2	rotating_nonsplit	0	0	FALSE
B3	rotating_nonsplit	0.1	0.1	TRUE

charybdis 2

Model	bhspin	mjlost	yrcsc	nbodyaverage	nbodyphase	nbodyvar	rmstab
C1	TRUE	FALSE	FALSE	FALSE	TRUE	TRUE	FALSE
C2	FALSE	FALSE	FALSE	FALSE	TRUE	TRUE	FALSE
C3	TRUE	FALSE	FALSE	TRUE	FALSE	FALSE	FALSE
C4	TRUE	TRUE	TRUE	FALSE	TRUE	TRUE	FALSE
C5	TRUE	TRUE	TRUE	FALSE	FALSE	FALSE	TRUE

energies of photons, and charged and neutral hadrons in a cone of radius of 0.4 (0.3) in the η–ϕ space centered on the muon (electron) candidate to the p_{T} of the lepton:

$$\mathcal{I} = \frac{(\sum_i E_{\mathrm{T}}^i) - E_{\mathrm{T}}^{\mathrm{PU}}}{p_{\mathrm{T}}^{\ell}}, \tag{5}$$

where the sum runs over charged hadrons originating from the hard-scattering vertex, neutral hadrons, and photons. The numerator of the ratio is corrected for contributions due to pileup ($E_{\mathrm{T}}^{\mathrm{PU}}$), using the fraction of energy carried by the charged hadrons originating from other vertices to estimate the contribution of neutral particles from pileup for muons, and an average area method [53], as estimated with FastJet for electrons. Muons (electrons) are required to have relative isolation values less than 0.15 (0.10).

Photons are required to have $p_{\mathrm{T}} > 50\,\mathrm{GeV}$ and to be in the same fiducial region as the electrons, and are reconstructed with a standard algorithm [47] using a medium working point. They are also required to be isolated, with the definition of isolation tuned to yield constant efficiency as a function of photon p_{T}. The pileup-corrected charged-hadron transverse energy sum within the isolation cone of radius of 0.3 is required to be less than 1.37 (1.10) GeV in the barrel (endcaps). A similarly defined neutral-hadron isolation sum is required to be less than $1.06\,\mathrm{GeV} + 0.014 p_{\mathrm{T}} + 0.000019\,\mathrm{GeV}^{-1} p_{\mathrm{T}}^2$ in the barrel and $2.69\,\mathrm{GeV} + 0.0139 p_{\mathrm{T}} + 0.000025\,\mathrm{GeV}^{-1} p_{\mathrm{T}}^2$ in the endcaps. Finally, the pileup-corrected isolation sum of any additional photon candidates in the isolation cone must be less than $0.28\,\mathrm{GeV} + 0.0053 p_{\mathrm{T}}$ ($0.39\,\mathrm{GeV} + 0.0034 p_{\mathrm{T}}$) in the barrel (endcaps).

5. Signal simulation

Signal events are simulated using dedicated MC event generators. For semiclassical BHs, the BlackMax v2.02.0 [56] and charybdis 2 v1.003 [57] generators are used, as summarized in Table 1 and detailed below. Quantum BHs are generated using the qbh v3.00 generator [28]. The fragmentation and hadronization of parton-level signal samples is done with pythia 8.205 [58], with the underlying event tune CUETP8M1 [59].

In the semiclassical case, several models are explored. We simulate the following scenarios: nonrotating BHs (models B1, C2), rotating BHs without energy loss (models B2, C1) and with an alternative evaporation model (C3), rotating BHs with 10% loss of mass and angular momentum (B3), rotating BHs with Yoshino–Rychkov bounds [60] (model C4), and rotating BHs with a stable remnant with the mass equal to the multidimensional Planck scale M_{D} (model C5, for which additionally the Charybdis2 parameter NBODY was changed from its default value of 2 to 0). The generator parameters used for semiclassical BH signal models are given in Table 1.

The parameters associated with the BH signal generation, as can be inferred from Eq. (3), are the number of extra dimensions n, the multidimensional Planck scale M_{D}, and the mass of the BH M_{BH}. For the semiclassical case, $n = 2$, 4, and 6, while M_{D} is varied between 2 and 9 TeV, and M_{BH} is varied in the range between M_{D} and 11 TeV. In the case of the QBHs, $n = 1$–6, while $M_{\mathrm{D}} = 2$–9 TeV and $M_{\mathrm{BH}} \geq M_{\mathrm{D}}$ with the upper bound kept at 11 TeV. For QBHs in the ADD model we use $n \geq 2$, while in the RS1 model n is restricted to 1.

String balls are generated using the charybdis 2 event generator for the nonrotating scenario. The number of extra dimensions is fixed at $n = 6$, as it was in earlier CMS publications. Note also that as the dependence of the SB dynamics on n is only implicit, via the relationship between the Planck and string scales. The mass of the string ball (M_{SB}) is varied between 5 and 10 TeV. Four different benchmark scenarios are considered:

- $M_{\mathrm{D}} = 5.93\,\mathrm{TeV}$, $M_{\mathrm{S}} = 1.1\,\mathrm{TeV}$, $g_{\mathrm{S}} = 0.2$;
- $M_{\mathrm{D}} = 5.36\,\mathrm{TeV}$, $M_{\mathrm{S}} = 1.1\,\mathrm{TeV}$, $g_{\mathrm{S}} = 0.3$;
- $M_{\mathrm{D}} = 6.80\,\mathrm{TeV}$, $M_{\mathrm{S}} = 1.5\,\mathrm{TeV}$, $g_{\mathrm{S}} = 0.4$;
- $M_{\mathrm{D}} = 8.57\,\mathrm{TeV}$, $M_{\mathrm{S}} = 2.0\,\mathrm{TeV}$, $g_{\mathrm{S}} = 0.5$.

These benchmarks are chosen such that the various regimes of the SB dynamics are probed, mainly between the first transition at $M_{\mathrm{SB}} = M_{\mathrm{S}}/g_{\mathrm{S}}$ and the BH transition at $M_{\mathrm{SB}} = M_{\mathrm{S}}/g_{\mathrm{S}}^2$. Above the second transition, SBs turn into semiclassical BHs, so the standard BH analysis fully applies. (We note that a significant fraction of the SB parameter space probed by the ATLAS Collaboration [33] in fact falls into the BH, and not the SB regime.) In all cases the fundamental Planck scale M_{D} is chosen to satisfy the matching condition at the SB/BH transition point: $\sigma_{\mathrm{BH}}(M_{\mathrm{S}}/g_{\mathrm{S}}^2) = \sigma_{\mathrm{SB}}(M_{\mathrm{S}}/g_{\mathrm{S}}^2) = 1/M_{\mathrm{S}}^2$, where $\sigma_{\mathrm{BH}}(M_{\mathrm{BH}})$ and $\sigma_{\mathrm{SB}}(M_{\mathrm{SB}})$ are the BH and SB parton-level production cross sections, as functions of their masses, respectively.

The choice of parton distribution functions (PDFs) used in this analysis was made as a result of detailed studies of the PDF dependence of signal cross sections. The leading order (LO) MSTW2008LO [61,62] PDFs are chosen for all the signal samples. This PDF set provides a conservative estimate of the signal cross section at high BH masses with respect to the modern NNPDF3.0 [63] PDFs. The cross section at large BH masses obtained with different PDF sets can vary up to an order of magnitude. The use of the MSTW2008LO PDF corresponds to the cross section at the lower edge of the uncertainty range for the NNPDF3.0 PDFs, therefore indicating a reasonable and conservative choice for signal simulation. The MSTW2008LO PDF has been recently superseded by the MMHT2014LO [64] set. However, a numerical comparison of the signal cross sections computed using both of these PDF sets reveals no differences. This is expected, as no new data constrain-

ing PDFs for processes with such high momentum transfer have been utilized in the global fit used to extract the MMHT2014LO PDF set. Given that MSTW2008LO was the PDF of choice for the Run 1 version of this analysis, the use of this PDF also allows one to directly compare Run 1 and Run 2 results.

The CMS detector simulation is performed using both detailed simulation via GEANT4 [65] (semiclassical BLACKMAX and CHARYBDIS 2 C1–C3 BH samples) and fast parametric simulation via the FASTSIM [66] package (QBH and SB samples, as well as CHARYBDIS 2 C4–C5 samples). The fast simulation samples are validated against the full simulation, and the small observed differences between the two approaches were found to have a negligible impact on the signal acceptance.

In addition we use simulated samples of W + jets, Z + jets, γ + jets, $t\bar{t}$, and QCD multijet events for auxiliary studies. These events are generated with the MADGRAPH5_AMC@NLO [67] event generator, followed by PYTHIA for description of hadronization and fragmentation. The NNPDF3.0 PDF set with the tune CUETP8M1 is used for the background generation, and the CMS detector response is simulated via GEANT4.

6. Backgrounds

The main SM backgrounds to the multiparticle final states from new-physics processes are QCD multijet and γ + jets production, vector bosons produced in association with jets (V + jets, where V stands for a W or Z boson), and $t\bar{t}$ process. The QCD multijet background is by far the dominant one. The additional backgrounds are not explicitly considered for the remainder of the analysis, as they together contribute only a few percent of the total background. They also have a very similar shape to the QCD multijet background, as evident from Fig. 1, which shows the comparison in the S_T distribution of the total contribution of all the simulated backgrounds and the data for both the low-multiplicity $N = 2$ and high-multiplicity $N \geq 6$ selections. While simulated samples are not used to estimate the background in this analysis, we note that the simulation nevertheless describes data reasonably well.

The background estimation strategy hinges on the shape of the S_T distribution in the tail region of the spectrum being independent of the object multiplicity. As a consequence of this invariance, the S_T distribution in higher multiplicity regions can be obtained by appropriately rescaling the low-multiplicity S_T spectrum, where signal contamination is expected to be minimal. Given the similarity of the shapes of the QCD multijet and other backgrounds, this technique also implicitly accounts for most of the contribution of the non-QCD backgrounds. The technique has been extensively validated in previous CMS publications [35–37], using both low-multiplicity data samples and simulated QCD multijet events.

The shape of the background is obtained by performing a binned likelihood fit of the S_T spectrum to a functional form given by $P_0(1+x)^{P_1}x^{-P_2-P_3\log(x)}$, where the P_i are free parameters of the fit, in the range between 1.4 and 2.4 TeV. The functional form used to fit the background is taken from earlier searches at the LHC and at the Fermilab Tevatron [68], and represents a well-established characterization of rapidly falling E_T spectra. Since the goal is to operate in the background-only control region for the extraction of these shapes or templates, the multiplicities chosen for the background extraction are $N = 2$ and 3. This choice is justified by the dedicated Run 2 analyses (e.g., [69]) as well as by the earlier iterations of this analysis (e.g., [70]) where no signal of new physics was observed in these low-multiplicity regions.

The background template extracted by fitting the S_T spectrum corresponding to the exclusive object multiplicity of $N = 2$ is normalized appropriately to obtain an estimate of the background for the S_T spectra at higher multiplicities. The normalization regions

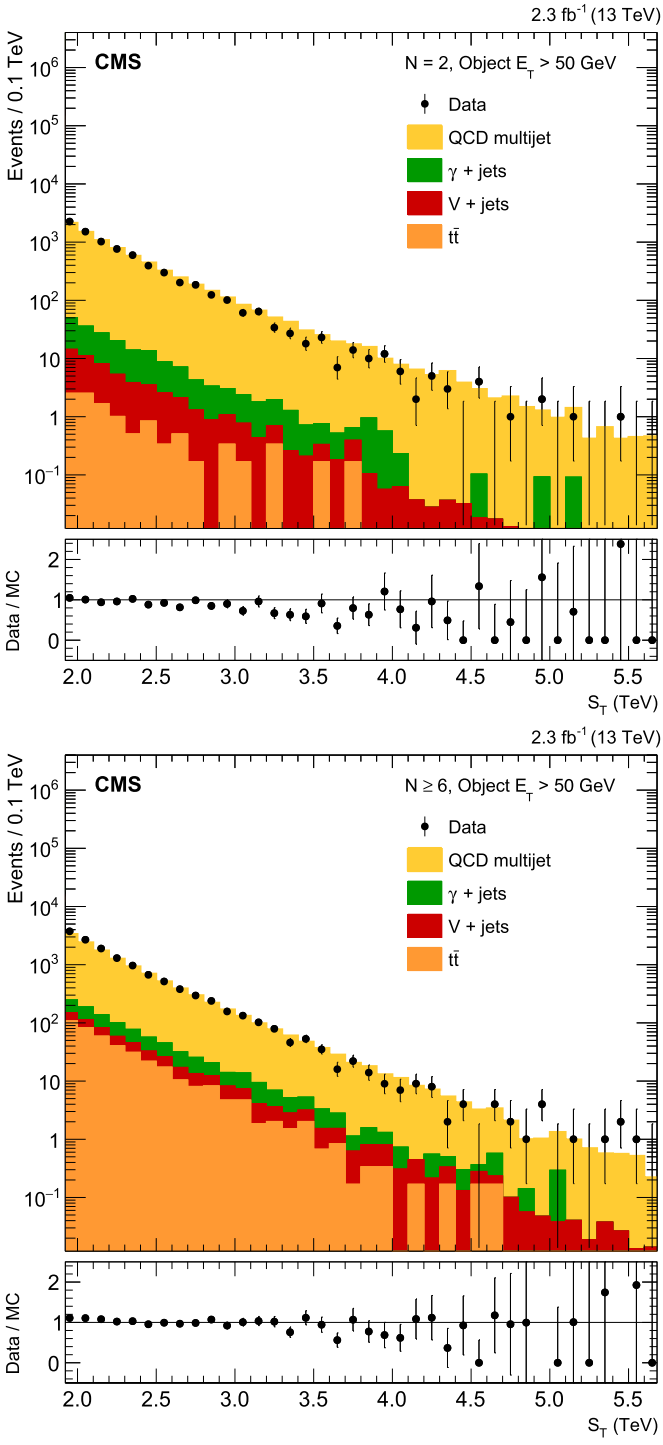

Fig. 1. Contributions of the main QCD multijet background, as well as γ + jets, V + jets (V = W, Z), and $t\bar{t}$ backgrounds to the S_T distribution for (top) exclusive multiplicity $N = 2$ and (bottom) inclusive multiplicity $N \geq 6$. All background predictions are based on simulated samples.

in S_T depend on the object multiplicity. Their definition is based on the studies of the S_T invariance in simulated QCD multijet samples. The lower S_T bound of the normalization region is chosen such that it is above the S_T turn-on region, while the choice of the upper S_T bound is guided by the need to operate in a regime of low signal contamination, namely where one does not expect a significant event yield for signals that have cross sections below those already excluded by the previous CMS search [37]. The

Table 2
The normalization regions and the corresponding $N = 2$ background template normalization factors s and their uncertainties for inclusive multiplicities, $N \geq 2 \ldots 10$. The normalization factor uncertainties are given by $s/\sqrt{N_{\mathrm{NR}}}$, where N_{NR} is the number of events in each normalization region.

Multiplicity	Normalization	
	Region [TeV]	Factor
$\geq$2	2.0–2.3	8.66 $\pm$ 0.15
$\geq$3	2.0–2.3	7.66 $\pm$ 0.13
$\geq$4	2.0–2.3	5.67 $\pm$ 0.10
$\geq$5	2.3–2.6	3.28 $\pm$ 0.09
$\geq$6	2.3–2.6	1.71 $\pm$ 0.05
$\geq$7	2.3–2.6	0.770 $\pm$ 0.022
$\geq$8	2.5–2.8	0.330 $\pm$ 0.013
$\geq$9	2.5–2.8	0.124 $\pm$ 0.005
$\geq$10	2.6–2.9	0.047 $\pm$ 0.002

normalization factors are calculated as the ratio of the number of data events in the normalization regions for the inclusive multiplicities of $N \geq 2 \ldots 10$ and that for the exclusive multiplicity of $N = 2$. These factors, along with the choice of the normalization region, are detailed in Table 2.

To ascertain the uncertainties associated with this method of background extraction, two additional fitting functions are considered, given by $P_0(P_1 + x)^{-P_2}$ and $P_0(P_1 + P_2 x + x^2)^{-P_3}$. With an aim to compute a conservative estimate of the uncertainty, both the $N = 2$ and 3 S_{T} spectra are used to estimate the background shape. This leads to six different functions used in the fit: one nominal and five additional ones that form an uncertainty envelope that is symmetrized around the main fit. The shape systematic uncertainty is indicated with the gray shaded bands in Figs. 2 and 3, which show the S_{T} spectrum observed in data for various inclusive multiplicities and the background predictions with their uncertainties. It ranges between 1 and 200% and rapidly increases in the high-S_{T} range because of the limited number of events in the $N = 2$ and 3 S_{T} spectra used to derive the background templates. We assign an additional 5% systematic uncertainty to address possible deviation from the S_{T} invariance by estimating the difference between the background predictions based on the $N = 2$ (default) and $N = 3$ templates. This is a subdominant uncertainty in the high-S_{T} range relevant for the analysis. The systematic uncertainties in the background estimate are detailed in Table 3 of Section 7.

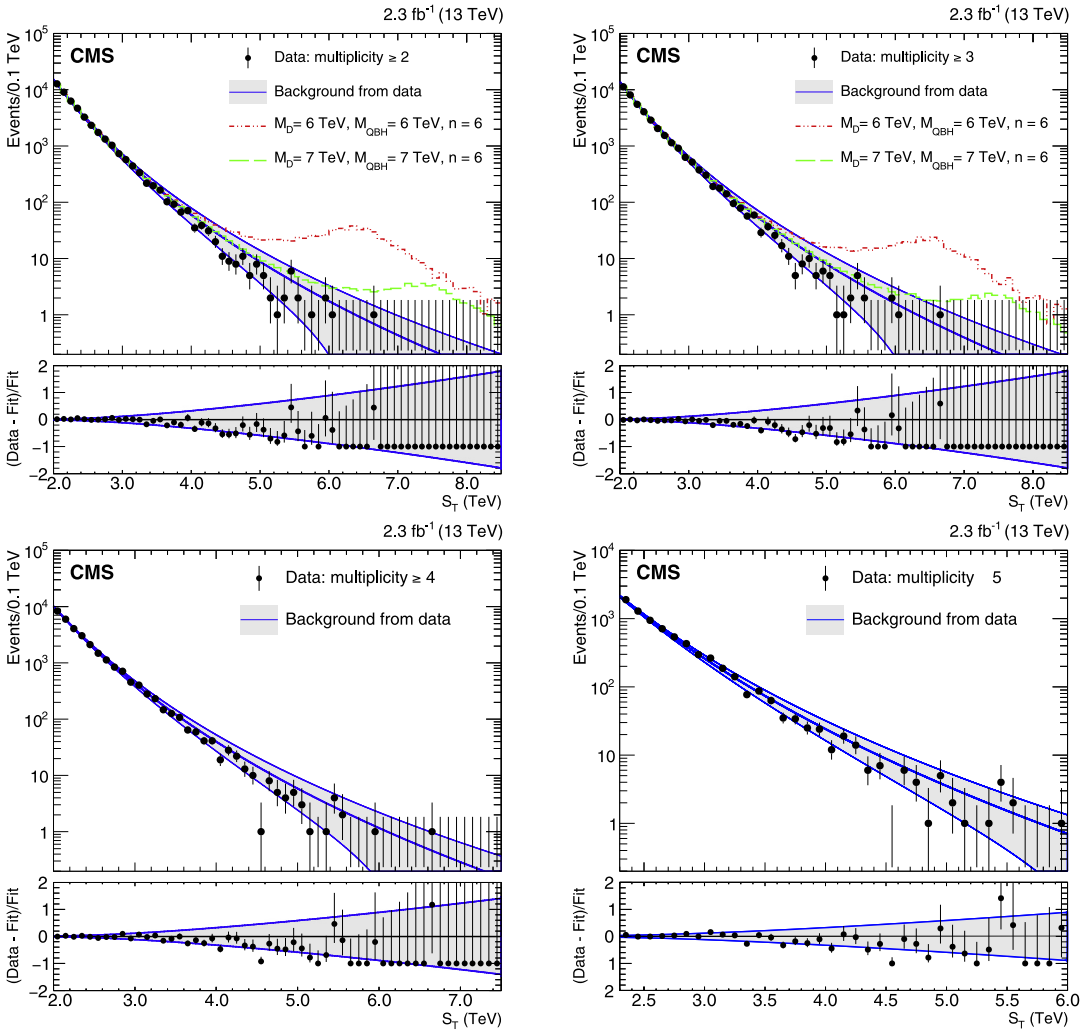

Fig. 2. The distributions of the total transverse energy, S_{T}, for inclusive multiplicities of objects (electrons, muons, photons, or jets) $N \geq 2, 3, 4, 5$. Observed data are shown by points with error bars, the solid blue lines along with the gray shaded band show the main background estimation (central blue line), along with the uncertainty band (outer blue lines). The deviation of the fit from the data is shown in each lower pane. The top two plots also show predictions for two quantum black hole benchmark scenarios added to the corresponding background predictions. (For interpretation of the references to color in this figure, the reader is referred to the web version of this article.)

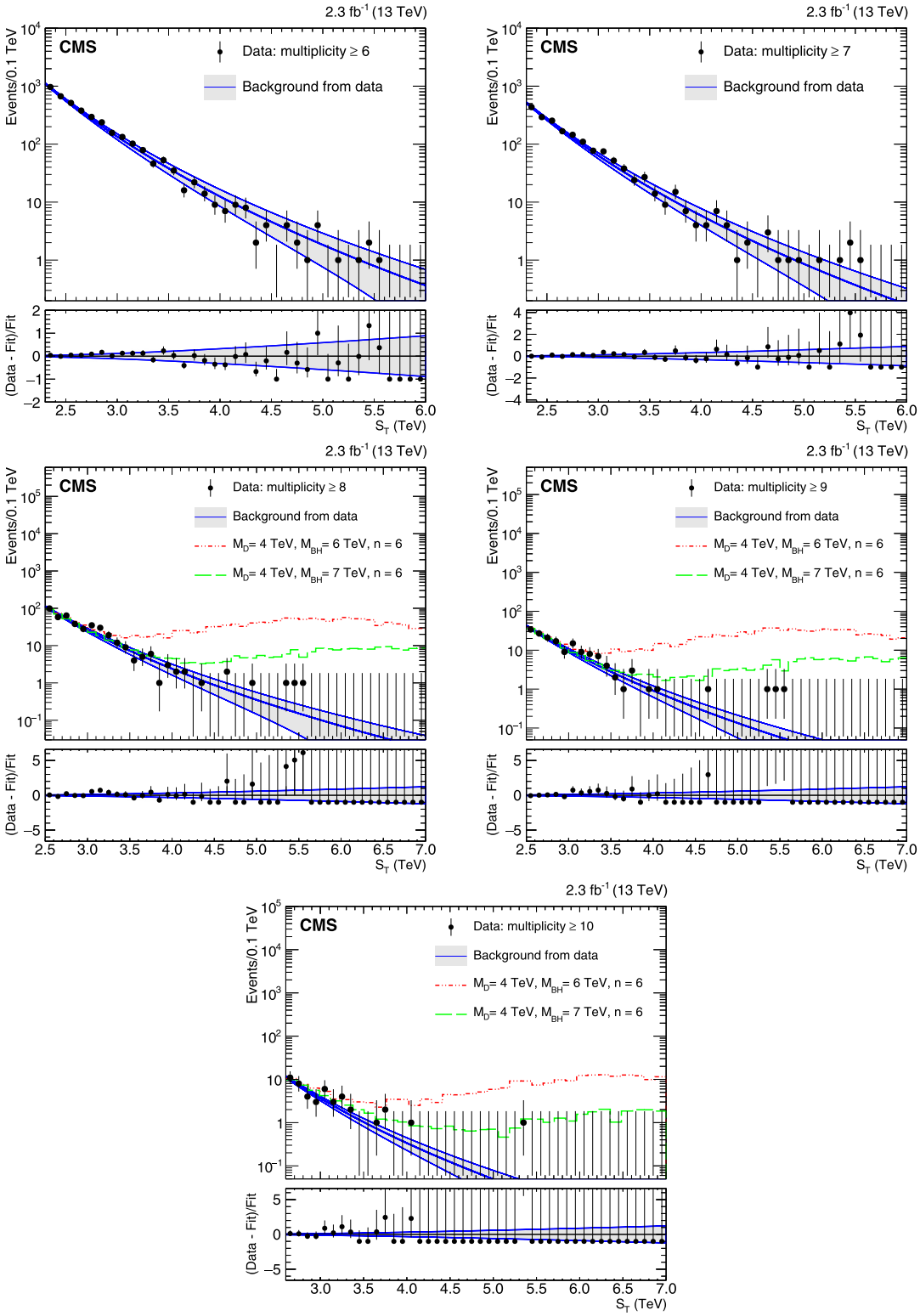

Fig. 3. The distributions of the total transverse energy, S_T, for inclusive multiplicities of objects (photons, muons, photons, or jets) $N \geq 6, 7, 8, 9, 10$. Observed data are shown by points with error bars, the solid blue lines along with the gray shaded band show the main background estimation (central blue line), along with the uncertainty band (outer blue lines). The deviation of the fit from the data is shown in each lower pane. The lower three plots also show predictions for two semiclassical black hole signal benchmarks added to the corresponding background predictions. (For interpretation of the references to color in this figure, the reader is referred to the web version of this article.)

Table 3
Summary of the systematic uncertainties. The range of the background uncertainties correspond to the S_T range probed. A dash implies that the corresponding uncertainty source does not apply.

Uncertainty	Effect on signal acceptance	Effect on background estimate
JES	±5%	–
JER	±4%	–
PDF	±6%	–
FSR	±1.2%	–
Integrated luminosity	±2.7%	–
Background normalization	–	±(0.5–5.2)%
Background shape	–	±(1–200)%,
Potential S_T noninvariance	–	±5%

As seen from Figs. 2 and 3, the data agree well with the predicted background and no evidence for new physics production is observed in any of the multiparticle final states studied.

7. Systematic uncertainties

A detailed study of the systematic uncertainties associated with this analysis was carried out, and these uncertainties were taken into account while computing exclusion limits, as detailed in Section 8. The dominant sources of systematic uncertainties arise from the effects of the jet energy scale (JES) and JER uncertainties, from the choice of the PDFs, and from the migration between event categories as a result of final-state radiation (FSR). The uncertainties vary for different signal samples and different inclusive multiplicities. The following sections give details on their estimation and the typical range for each uncertainty.

7.1. Parton distribution functions

There are two different sources of the PDF uncertainty that could affect the signal acceptance. The uncertainty could simply come from the choice of the PDF set. Alternatively, the systematic uncertainty could come from the variations induced by the uncertainties associated with the fit parameters in a chosen PDF set. The latter uncertainty is estimated by calculating $2k+1$ weights per event, where k is the number of alternative PDF sets with parameters varied within their associated uncertainties either up or down. These alternative sets are provided by the authors of each PDF set, along with the main PDFs used in the signal generation. The signal acceptance is then calculated for each of these weights, resulting in $2k+1$ values of the acceptance. For a particular choice of PDF set, the systematic uncertainty in the acceptance is quoted as the sum in quadrature of the deviations from the central value for each of the k PDF eigenvectors. This analysis is further extended by using various PDFs, such as MSTW2008LO, CTEQ6.1L [71], and CT10 [72]. The uncertainty is computed for a particular benchmark scenario, a nonrotating BH with $M_D = 3$ TeV, $M_{BH} = 5.5$ TeV, and $n = 2$, representative of the uncertainties for other benchmark points in the range probed by this analysis. The uncertainty in the acceptance using the variation of the chosen PDF, MSTW2008LO, does not exceed 0.5%. The uncertainty due to the choice of the PDF is significantly larger and can be as high as 6%. Following the recommendations of the PDF4LHC group [73,74], we assign a total uncertainty of 6% associated with this source of the systematic uncertainty.

7.2. Jet energy scale and resolution

The CMS experiment has adopted a factorized approach [51,52] to the application of corrections associated with the energy of a jet. After the subtraction of the additional energy due to pileup, the energies of the reconstructed jets are corrected for the nonlinear response of the calorimeter. These corrections are parametrized in p_T and η, and are derived from simulation and in situ measurements of the energy balance in dijet, multijet, γ + jet, and leptonic Z + jet events [51,52]. Given the predominance of jets in the final state of interest, the uncertainty related to the JES can significantly affect the signal acceptance. The JES is modified by one standard deviation in both upward and downward directions, and the corresponding changes in the jet energies are propagated into the E_T^{miss} and S_T computation. For various model-specific scenarios, we find the variation to lie between 1 and 5% and conservatively assign a uniform uncertainty in signal acceptance of 5% due to the JES uncertainty.

The uncertainty due to the JER is estimated by oversmearing jet energies in simulated signal samples with η-dependent factors to match the resolution observed in data. The effect of this change to the jet energy is propagated to the E_T^{miss} and S_T calculations. The JER uncertainty in the signal acceptance varies between 1.2 and 4.0%; we therefore assign a conservative uniform uncertainty of 4% to account for this effect.

In estimating both the JES and JER uncertainties, we find that there are migrations of events in different multiplicity categories due to the jet p_T values moving either above or below the 50 GeV threshold. The respective values of uncertainties associated with both of these sources sufficiently cover the effect of event migration. These two uncertainties affect only the simulated signal yields, as the background determination does not rely on simulation.

7.3. Final-state radiation

The presence of imperfectly modeled FSR may result in event migration between various multiplicity bins due to the change in the number of objects counted toward the S_T. The uncertainty in the signal acceptance due to the imperfect modeling of FSR is estimated by varying the parameters in the PYTHIA 8 generator that govern FSR modeling, and is found to be 1.2%.

The sources of systematic uncertainties considered in the analysis and their magnitude are listed in Table 3.

In addition, an uncertainty in the integrated luminosity of 2.7% [75] is propagated to both the model-independent and model-specific limits. All other uncertainties are negligible [35–37].

8. Model-independent limits

No statistically significant deviations of data relative to the background predictions are observed in any of the spectra. Exclusion limits on various signals are set using the modified frequentist CL_s approach [76,77] with the profile likelihood as a test statistic and nuisance parameters implemented via log-normal priors. The likelihood of the observed number of events is modeled with a Poisson distribution. The limit calculation is performed using the methodology developed by the ATLAS and CMS Collaborations in the search for the Higgs boson [78]. The systematic uncertainties taken into account are detailed in Section 7.

As mentioned in Section 1, the main emphasis of the analysis is the computation of model-independent limits on the product of the hypothetical signal cross section and acceptance (σA) in inclusive $N \geq N^{min}$ multiplicity bins, as a function of the minimum S_T requirement (S_T^{min}). These limits represent the minimum σA of a potential signal excluded by the analysis and do not assume any particular signal model. This makes the limits applicable to a large variety of BH models and other theoretical models with processes that result in high-multiplicity final states. To obtain the model-independent limits, a counting experiment is performed for

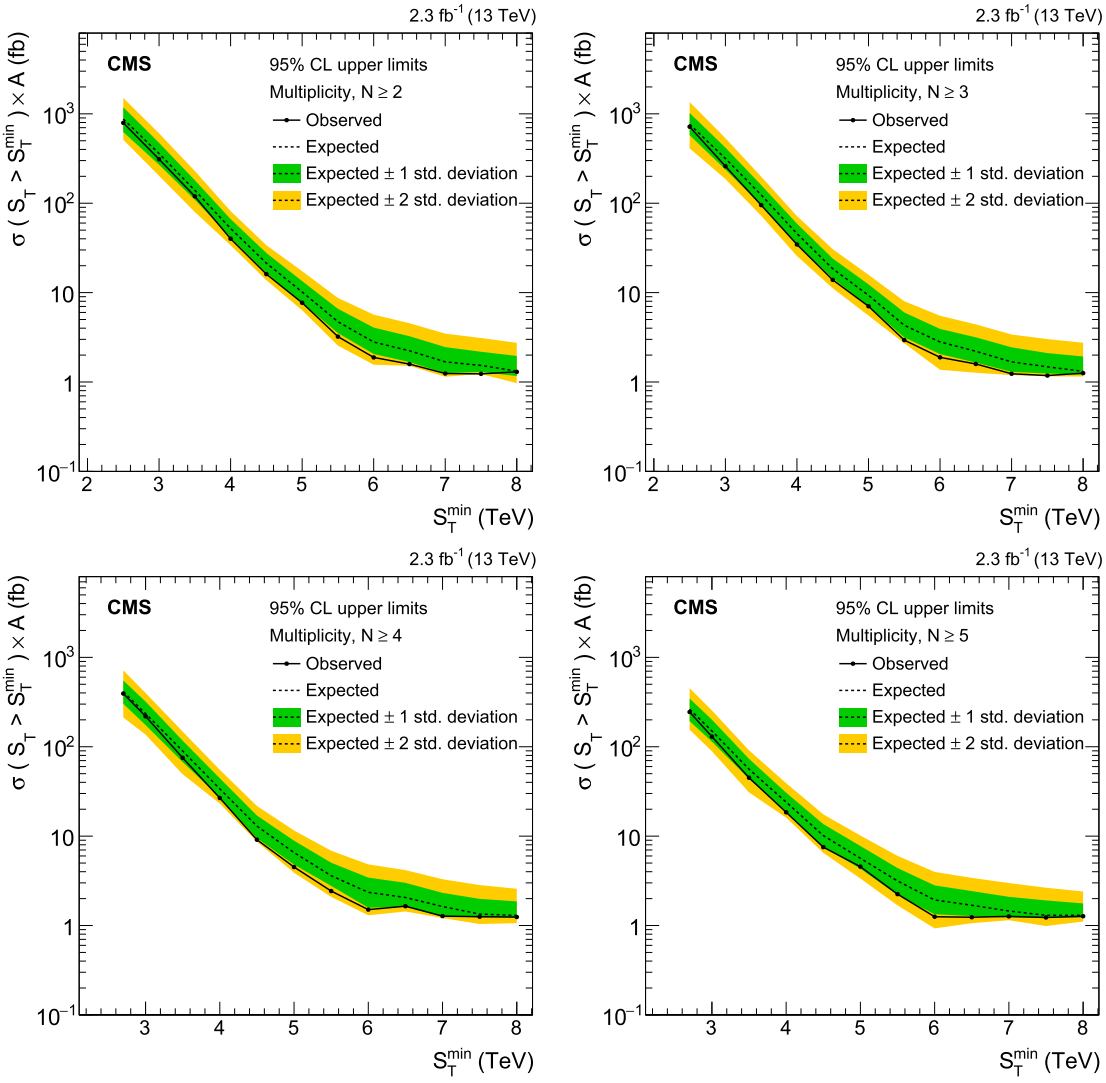

Fig. 4. Model-independent 95% CL upper limits on the cross section times acceptance for four sets of inclusive multiplicity thresholds: $N \geq 2$, 3, 4, and 5. Observed (expected) limits are shown as solid (dashed) lines, and the two bands correspond to ± 1 and 2 standard deviations in the expected limit.

$N \geq N^{\min}$ and $S_T > S_T^{\min}$. These limits, at 95% confidence level (CL), are presented in Figs. 4 and 5 for $N^{\min} \geq 2, \ldots, 10$. The limits on σA approach 1.3 fb at high values of $S_T^{\min}$.

Model-independent limits can be used straightforwardly to test any model of new physics that predicts signal corresponding to high-multiplicity, energetic final states. Given that the object selection efficiency is close to 100%, all is needed to test a particular model against the results of this search is to estimate the signal acceptance as a function of the minimum S_T requirement, corresponding to the selections described in Section 4, which can be done with sufficient precision even at the generator level. A comparison of the product of the signal cross section and the acceptance as a function of the minimum S_T requirement with the model-independent limit at the relevant object multiplicity would then indicate whether a particular model has been excluded by this analysis.

9. Model-specific limits

In the case of the model-specific limits, the selection criteria ($N^{\min}$, $S_T^{\min}$) were chosen for optimum sensitivity to each particular model. This was done by using the lowest value of the expected limit, as well as the maximum value of the Z_{bi} [79] statistic, and converting the corresponding model-independent limit into a limit on the BH or SB mass, using the known signal cross section and acceptance. The Z_{bi} statistic is a measure of equivalent Gaussian signal significance obtained by considering the binomial probability of the events in data being distributed at least as signal-like as observed, under the assumption of the background-only hypothesis. In the majority of cases, the limit- and significance-based optimizations are in agreement and lead to the same set of optimum selection requirements. Since the signal MC benchmark points were produced on a grid of discrete M_{BH} values (with a typical spacing of 1 TeV), in order to obtain the mass limit, we smoothly interpolate the signal cross section times acceptance and the exclusion limit between the adjacent points on the grid. Typical precision of this procedure expressed as a limit on the minimum BH mass is ~0.1 TeV, although for some of the points where the grid spacing was not as fine, the precision can be somewhat worse.

Model-specific limits span the entire set of models discussed in Section 5. The limits on semiclassical BHs in all cases, except for the model with stable remnant (C5), come from the optimized values of $N^{\min}$ equal to 9 or 10 for low BH masses and from lower

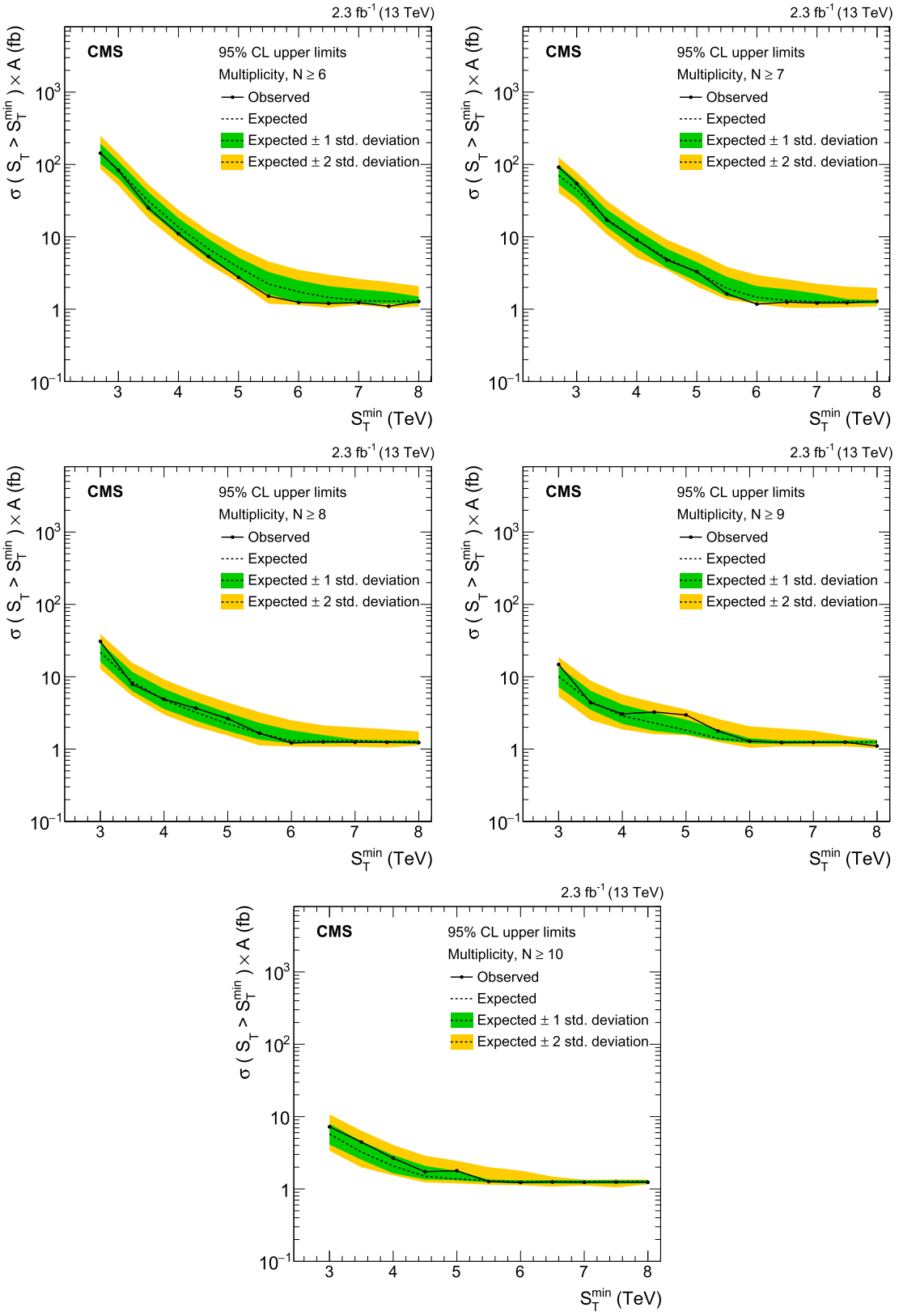

Fig. 5. Model-independent 95% CL upper limits on the cross section times acceptance for five sets of inclusive multiplicity thresholds: $N \geq 6$, 7, 8, 9, and 10. Observed (expected) limits are shown as a solid (dashed) lines, and the two bands correspond to ± 1 and 2 standard deviations in the expected limit.

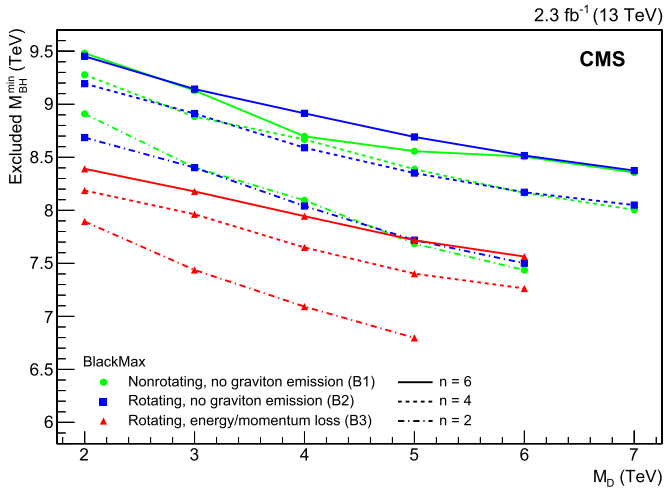

Fig. 6. The 95% CL lower limits on the minimum semiclassical black hole mass as a function of the Planck scale M_D, for several benchmark models generated with BLACKMAX: nonrotating and rotating black holes without graviton emission and rotating black holes with energy-momentum loss.

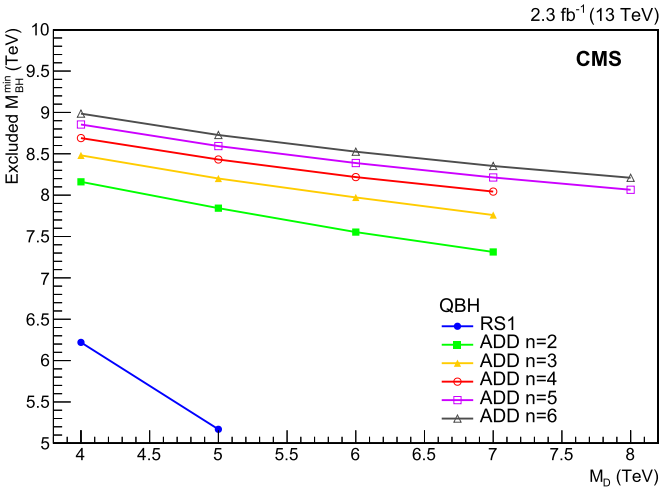

Fig. 8. The 95% CL lower limits on minimum quantum black hole mass as a function of the Planck scale M_D, for several benchmark models. The blue (lower) line corresponds to quantum black holes in the RS1 model; while the other lines correspond to the ADD model for the number of extra dimensions $n = 2, \ldots, 6$.

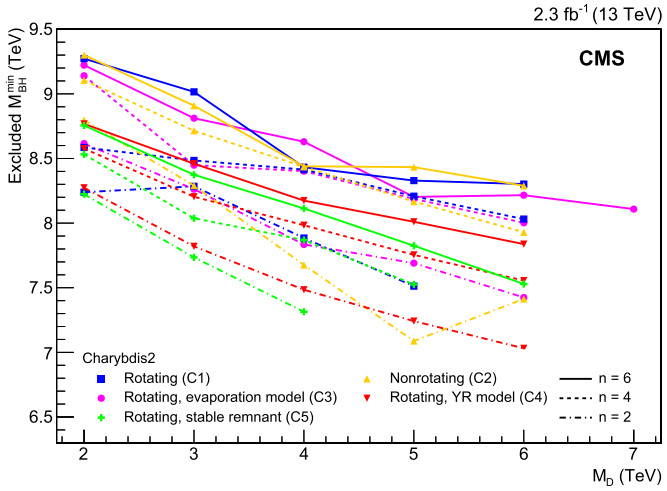

Fig. 7. The 95% CL lower limits on minimum semiclassical black hole mass as a function of the Planck scale M_D, for several benchmark models generated with CHARYBDIS 2: rotating and nonrotating black holes, rotating black holes with an alternative evaporation model, rotating black holes with Yoshino–Rychkov bounds, and rotating black holes with a stable remnant.

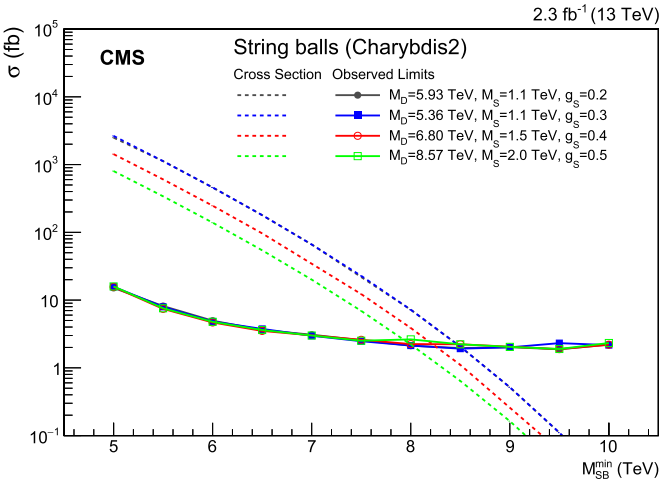

Fig. 9. The 95% CL upper limits on the cross section for the production of string balls and the corresponding theoretical cross sections. The solid colored lines correspond to the observed cross section limits; the dashed colored curves correspond to theoretical cross sections.

values of $N^{\min}$ for high BH masses, thanks to smaller backgrounds at high values of S_T. In Fig. 6, we show the observed lower limits on the semiclassical BH mass at 95% CL for BLACKMAX signal samples. In these models, we exclude minimum BHs masses below 7.0–9.5 TeV, for a large set of model parameters. Similar limits for models generated with the CHARYBDIS 2 generator are shown in Fig. 7. Considering that an independent optimization was used for each model, and for each M_D and n point, these limits are in general agreement with those obtained using BLACKMAX for analogous models. The limits significantly extend those from LHC Run 1 [37], which only reach 6.5 TeV.

In the case of QBHs and the case of semiclassical BHs with a stable remnant, where the number of produced particles is small as the massive stable remnant escapes detection, the best sensitivity is achieved for $N^{\min} = 2$. This sample partially overlaps with the $N = 2$ data set used for deriving the background template. Nevertheless, even in this case we still can use the background estimate based on the $N = 2$ spectrum, because the background is determined using only the low-S_T range of the spectrum (1.4–2.4 TeV), where the signal has already been excluded up to ≈5 TeV by the 8 TeV analysis [37]. Thus the potential signal contamination of the S_T range used in deriving the background shape and normalization is negligible.

The lower limits on the minimum QBH mass are shown in Fig. 8 and span the 7.3–9.0 TeV range for the ADD ($n > 2$) and 5.1–6.2 TeV range for the RS1 ($n = 1$) QBHs. Again, these limits extend significantly those obtained in the LHC Run 1 (4.6–6.2 TeV).

Finally, for the case of the SBs, the mass exclusion limits shown in Fig. 9 reach 8.0–8.5 TeV. Most of these limits correspond to the saturated string ball regime, $M_S/g_S < M_{SB} < M_S/g_S^2$. The transitions between the saturated SB and BH regimes are not clearly visible in theoretical cross section curves, as the parton-level cross section that exhibits this transition as a change in slope is significantly modified by the rapidly falling PDFs.

10. Summary

We have conducted a search for new physics in multiparticle final states in a data sample of proton–proton collisions at $\sqrt{s} =$

13 TeV collected with the CMS detector, corresponding to an integrated luminosity of 2.3 fb^{-1}. The discriminating variable between signal and the dominant QCD multijet background is the scalar sum of the transverse energies of all reconstructed objects in the event, S_T. The shape of the S_T distribution in low-multiplicity data is used to predict the QCD multijet background in high-multiplicity signal regions. No significant excess of events over the standard model expectation is observed in any of the analyzed final-state multiplicities. Comparing the S_T distribution in data with that from the background prediction, we set model-independent upper limits at 95% confidence level on the product of the cross section and the acceptance for hypothetical signals. In addition, we set limits on various theoretical black hole and string ball models, including models of rotating and nonrotating black holes and quantum black holes. In all cases the exclusions represent significant improvements over the limits achieved in Run 1 of the LHC.

Acknowledgements

We congratulate our colleagues in the CERN accelerator departments for the excellent performance of the LHC and thank the technical and administrative staffs at CERN and at other CMS institutes for their contributions to the success of the CMS effort. In addition, we gratefully acknowledge the computing centers and personnel of the Worldwide LHC Computing Grid for delivering so effectively the computing infrastructure essential to our analyses. Finally, we acknowledge the enduring support for the construction and operation of the LHC and the CMS detector provided by the following funding agencies: BMWFW and FWF (Austria); FNRS and FWO (Belgium); CNPq, CAPES, FAPERJ, and FAPESP (Brazil); MES (Bulgaria); CERN; CAS, MoST, and NSFC (China); COLCIENCIAS (Colombia); MSES and CSF (Croatia); RPF (Cyprus); SENESCYT (Ecuador); MoER, ERC IUT, and ERDF (Estonia); Academy of Finland, MEC, and HIP (Finland); CEA and CNRS/IN2P3 (France); BMBF, DFG, and HGF (Germany); GSRT (Greece); OTKA and NIH (Hungary); DAE and DST (India); IPM (Iran); SFI (Ireland); INFN (Italy); MSIP and NRF (Republic of Korea); LAS (Lithuania); MOE and UM (Malaysia); BUAP, CINVESTAV, CONACYT, LNS, SEP, and UASLP-FAI (Mexico); MBIE (New Zealand); PAEC (Pakistan); MSHE and NSC (Poland); FCT (Portugal); JINR (Dubna); MON, RosAtom, RAS, RFBR and RAEP (Russia); MESTD (Serbia); SEIDI, CPAN, PCTI and FEDER (Spain); Swiss Funding Agencies (Switzerland); MST (Taipei); ThEPCenter, IPST, STAR, and NSTDA (Thailand); TUBITAK and TAEK (Turkey); NASU and SFFR (Ukraine); STFC (United Kingdom); DOE and NSF (USA).

Individuals have received support from the Marie-Curie program and the European Research Council and EPLANET (European Union); the Leventis Foundation; the A. P. Sloan Foundation; the Alexander von Humboldt Foundation; the Belgian Federal Science Policy Office; the Fonds pour la Formation à la Recherche dans l'Industrie et dans l'Agriculture (FRIA-Belgium); the Agentschap voor Innovatie door Wetenschap en Technologie (IWT-Belgium); the Ministry of Education, Youth and Sports (MEYS) of the Czech Republic; the Council of Science and Industrial Research, India; the HOMING PLUS program of the Foundation for Polish Science, cofinanced from European Union, Regional Development Fund, the Mobility Plus program of the Ministry of Science and Higher Education, the National Science Center (Poland), contracts Harmonia 2014/14/M/ST2/00428, Opus 2014/13/B/ST2/02543, 2014/15/B/ST2/03998, and 2015/19/B/ST2/02861, Sonata-bis 2012/07/E/ST2/01406; the National Priorities Research Program by Qatar National Research Fund; the Programa Clarín-COFUND del Principado de Asturias; the Thalis and Aristeia programs cofinanced by EU-ESF and the Greek NSRF; the Rachadapisek Sompot Fund for Postdoctoral Fellowship, Chulalongkorn University and the Chulalongkorn Academic into Its 2nd Century Project Advancement Project (Thailand); and the Welch Foundation, contract C-1845.

References

[1] S.L. Glashow, Partial symmetries of weak interactions, Nucl. Phys. 22 (1961) 579, http://dx.doi.org/10.1016/0029-5582(61)90469-2.
[2] S. Weinberg, A model of leptons, Phys. Rev. Lett. 19 (1967) 1264, http://dx.doi.org/10.1103/PhysRevLett.19.1264.
[3] A. Salam, Weak and electromagnetic interactions, in: N. Svartholm (Ed.), Elementary Particle Physics: Relativistic Groups and Analyticity. Proceedings of the Eighth Nobel Symposium, Almqvist & Wiksell, Stockholm, 1968, p. 367.
[4] R. Barbieri, G.F. Giudice, Upper bounds on supersymmetric particle masses, Nucl. Phys. B 306 (1988) 63, http://dx.doi.org/10.1016/0550-3213(88)90171-X.
[5] G.R. Farrar, P. Fayet, Phenomenology of the production, decay, and detection of new hadronic states associated with supersymmetry, Phys. Lett. B 76 (1978) 575, http://dx.doi.org/10.1016/0370-2693(78)90858-4.
[6] S.P. Martin, A supersymmetry primer, in: G.L. Kane (Ed.), Perspectives on Supersymmetry II, in: Adv. Ser. Dir. High Energy Phys., vol. 21, World Scientific, 2010, p. 1, arXiv:hep-ph/9709356.
[7] J.A. Evans, Y. Kats, D. Shih, M.J. Strassler, Toward full LHC coverage of natural supersymmetry, J. High Energy Phys. 07 (2014) 101, http://dx.doi.org/10.1007/JHEP07(2014)101, arXiv:1310.5758.
[8] S. Dimopoulos, L. Susskind, Mass without scalars, Nucl. Phys. B 155 (1979) 237, http://dx.doi.org/10.1016/0550-3213(79)90364-X, 2,930(1979).
[9] P.H. Frampton, S.L. Glashow, Chiral color: an alternative to the standard model, Phys. Lett. B 190 (1987) 157, http://dx.doi.org/10.1016/0370-2693(87)90859-8.
[10] C.T. Hill, Topcolor: top quark condensation in a gauge extension of the standard model, Phys. Lett. B 266 (1991) 419, http://dx.doi.org/10.1016/0370-2693(91)91061-Y.
[11] C.T. Hill, S.J. Parke, Top production: sensitivity to new physics, Phys. Rev. D 49 (1994) 4454, http://dx.doi.org/10.1103/PhysRevD.49.4454, arXiv:hep-ph/9312324.
[12] R.S. Chivukula, A.G. Cohen, E.H. Simmons, New strong interactions at the Tevatron?, Phys. Lett. B 380 (1996) 92, http://dx.doi.org/10.1016/0370-2693(96)00464-9, arXiv:hep-ph/9603311.
[13] E.H. Simmons, Coloron phenomenology, Phys. Rev. D 55 (1997) 1678, http://dx.doi.org/10.1103/PhysRevD.55.1678, arXiv:hep-ph/9608269.
[14] N. Arkani-Hamed, S. Dimopoulos, G.R. Dvali, The hierarchy problem and new dimensions at a millimeter, Phys. Lett. B 429 (1998) 263, http://dx.doi.org/10.1016/S0370-2693(98)00466-3, arXiv:hep-ph/9803315.
[15] I. Antoniadis, N. Arkani-Hamed, S. Dimopoulos, G.R. Dvali, New dimensions at a millimeter to a fermi and superstrings at a TeV, Phys. Lett. B 436 (1998) 257, http://dx.doi.org/10.1016/S0370-2693(98)00860-0, arXiv:hep-ph/9804398.
[16] N. Arkani-Hamed, S. Dimopoulos, G.R. Dvali, Phenomenology, astrophysics and cosmology of theories with submillimeter dimensions and TeV scale quantum gravity, Phys. Rev. D 59 (1999) 086004, http://dx.doi.org/10.1103/PhysRevD.59.086004, arXiv:hep-ph/9807344.
[17] L. Randall, R. Sundrum, A large mass hierarchy from a small extra dimension, Phys. Rev. Lett. 83 (1999) 3370, http://dx.doi.org/10.1103/PhysRevLett.83.3370, arXiv:hep-ph/9905221.
[18] L. Randall, R. Sundrum, An alternative to compactification, Phys. Rev. Lett. 83 (1999) 4690, http://dx.doi.org/10.1103/PhysRevLett.83.4690, arXiv:hep-th/9906064.
[19] S. Dimopoulos, G.L. Landsberg, Black holes at the LHC, Phys. Rev. Lett. 87 (2001) 161602, http://dx.doi.org/10.1103/PhysRevLett.87.161602, arXiv:hep-ph/0106295.
[20] S.B. Giddings, S.D. Thomas, High energy colliders as black hole factories: the end of short distance physics, Phys. Rev. D 65 (2002) 056010, http://dx.doi.org/10.1103/PhysRevD.65.056010, arXiv:hep-ph/0106219.
[21] L.A. Anchordoqui, H. Goldberg, A.D. Shapere, Phenomenology of Randall–Sundrum black holes, Phys. Rev. D 66 (2002) 024033, http://dx.doi.org/10.1103/PhysRevD.66.024033, arXiv:hep-ph/0204228.
[22] G.L. Landsberg, Black holes at future colliders and beyond, J. Phys. G 32 (2006) R337, http://dx.doi.org/10.1088/0954-3899/32/9/R02, arXiv:hep-ph/0607297.
[23] P. Meade, L. Randall, Black holes and quantum gravity at the LHC, J. High Energy Phys. 05 (2008) 003, http://dx.doi.org/10.1088/1126-6708/2008/05/003, arXiv:0708.3017.
[24] R.C. Myers, M.J. Perry, Black holes in higher dimensional space-times, Ann. Phys. 172 (1986) 304, http://dx.doi.org/10.1016/0003-4916(86)90186-7.
[25] S.W. Hawking, Particle creation by black holes, Commun. Math. Phys. 43 (1975) 199, http://dx.doi.org/10.1007/BF02345020, Erratum: http://dx.doi.org/10.1007/BF01608497.
[26] X. Calmet, W. Gong, S.D.H. Hsu, Colorful quantum black holes at the LHC, Phys. Lett. B 668 (2008) 20, http://dx.doi.org/10.1016/j.physletb.2008.08.011, arXiv:0806.4605.

[27] D.M. Gingrich, Quantum black holes with charge, color and spin at the LHC, J. Phys. G 37 (2010) 105008, http://dx.doi.org/10.1088/0954-3899/37/10/105008, arXiv:0912.0826.

[28] D.M. Gingrich, Monte Carlo event generator for black hole production and decay in proton–proton collisions – QBH version 1.02, Comput. Phys. Commun. 181 (2010) 1917, http://dx.doi.org/10.1016/j.cpc.2010.07.027, arXiv:0911.5370.

[29] S. Dimopoulos, R. Emparan, String balls at the LHC and beyond, Phys. Lett. B 526 (2002) 393, http://dx.doi.org/10.1016/S0370-2693(01)01525-8, arXiv:hep-ph/0108060.

[30] R. Hagedorn, Statistical thermodynamics of strong interactions at high-energies, Suppl. Nuovo Cim. 3 (1965) 147.

[31] G. Landsberg, Black holes at the Large Hadron Collider, Fundam. Theor. Phys. 178 (2015) 267, http://dx.doi.org/10.1007/978-3-319-10852-0_9.

[32] ATLAS Collaboration, Search for new phenomena in dijet mass and angular distributions from pp collisions at $\sqrt{s} = 13$ TeV with the ATLAS detector, Phys. Lett. B 754 (2016) 302, http://dx.doi.org/10.1016/j.physletb.2016.01.032, arXiv:1512.01530.

[33] ATLAS Collaboration, Search for strong gravity in multijet final states produced in pp collisions at $\sqrt{s} = 13$ TeV using the ATLAS detector at the LHC, J. High Energy Phys. 03 (2016) 026, http://dx.doi.org/10.1007/JHEP03(2016)026, arXiv:1512.02586.

[34] ATLAS Collaboration, Search for TeV-scale gravity signatures in high-mass final states with leptons and jets with the ATLAS detector at $\sqrt{s} = 13$ TeV, Phys. Lett. B 760 (2016) 520, http://dx.doi.org/10.1016/j.physletb.2016.07.030, arXiv:1606.02265.

[35] CMS Collaboration, Search for microscopic black hole signatures at the Large Hadron Collider, Phys. Lett. B 697 (2011) 434, http://dx.doi.org/10.1016/j.physletb.2011.02.032, arXiv:1012.3375.

[36] CMS Collaboration, Search for microscopic black holes in pp collisions at $\sqrt{s} = 7$ TeV, J. High Energy Phys. 04 (2012) 061, http://dx.doi.org/10.1007/JHEP04(2012)061, arXiv:1202.6396.

[37] CMS Collaboration, Search for microscopic black holes in pp collisions at $\sqrt{s} = 8$ TeV, J. High Energy Phys. 07 (2013) 178, http://dx.doi.org/10.1007/JHEP07(2013)178, arXiv:1303.5338.

[38] CMS Collaboration, Search for stealth supersymmetry in events with jets, either photons or leptons, and low missing transverse momentum in pp collisions at 8 TeV, Phys. Lett. B 743 (2015) 503, http://dx.doi.org/10.1016/j.physletb.2015.03.017, arXiv:1411.7255.

[39] CMS Collaboration, Search for new physics in events with high jet multiplicity and low missing transverse momentum in proton–proton collisions at $\sqrt{s} = 8$ TeV, Phys. Lett. B 770 (2017) 257, http://dx.doi.org/10.1016/j.physletb.2017.01.073, arXiv:1608.01224.

[40] ATLAS Collaboration, Search for TeV-scale gravity signatures in final states with leptons and jets with the ATLAS detector at $\sqrt{s} = 7$ TeV, Phys. Lett. B 716 (2013) 122, http://dx.doi.org/10.1016/j.physletb.2012.08.009, arXiv:1204.4646.

[41] ATLAS Collaboration, Search for microscopic black holes and string balls in final states with leptons and jets with the ATLAS detector at $\sqrt{s} = 8$ TeV, J. High Energy Phys. 08 (2014) 103, http://dx.doi.org/10.1007/JHEP08(2014)103, arXiv:1405.4254.

[42] ATLAS Collaboration, Search for low-scale gravity signatures in multi-jet final states with the ATLAS detector at $\sqrt{s} = 8$ TeV, J. High Energy Phys. 07 (2015) 032, http://dx.doi.org/10.1007/JHEP07(2015)032, arXiv:1503.08988.

[43] CMS Collaboration, Description and performance of track and primary-vertex reconstruction with the CMS tracker, J. Instrum. 9 (2014) P10009, http://dx.doi.org/10.1088/1748-0221/9/10/P10009, arXiv:1405.6569.

[44] CMS Collaboration, The CMS trigger system, J. Instrum. 12 (2017) P01020, http://dx.doi.org/10.1088/1748-0221/12/01/P01020.

[45] CMS Collaboration, The CMS experiment at the CERN LHC, J. Instrum. 3 (2008) S08004, http://dx.doi.org/10.1088/1748-0221/3/08/S08004.

[46] CMS Collaboration, Particle-flow reconstruction and global event description with the CMS detector, arXiv:1706.04965, 2017, submitted to JINST.

[47] CMS Collaboration, Performance of photon reconstruction and identification with the CMS detector in proton–proton collisions at $\sqrt{s} = 8$ TeV, J. Instrum. 10 (2015) P08010, http://dx.doi.org/10.1088/1748-0221/10/08/P08010, arXiv:1502.02702.

[48] CMS Collaboration, Performance of the CMS missing transverse momentum reconstruction in pp data at $\sqrt{s} = 8$ TeV, J. Instrum. 10 (2015) P02006, http://dx.doi.org/10.1088/1748-0221/10/02/P02006, arXiv:1411.0511.

[49] M. Cacciari, G.P. Salam, G. Soyez, The anti-k_t jet clustering algorithm, J. High Energy Phys. 04 (2008) 063, http://dx.doi.org/10.1088/1126-6708/2008/04/063, arXiv:0802.1189.

[50] M. Cacciari, G.P. Salam, G. Soyez, FastJet user manual, Eur. Phys. J. C 72 (2012) 1896, http://dx.doi.org/10.1140/epjc/s10052-012-1896-2, arXiv:1111.6097.

[51] CMS Collaboration, Determination of jet energy calibration and transverse momentum resolution in CMS, J. Instrum. (2011) P11002, http://dx.doi.org/10.1088/1748-0221/6/11/P11002, arXiv:1107.4277.

[52] CMS Collaboration, Jet energy scale and resolution in the CMS experiment in pp collisions at 8 TeV, J. Instrum. (2017) P02014, http://dx.doi.org/10.1088/1748-0221/12/02/P02014, arXiv:1607.03663.

[53] M. Cacciari, G.P. Salam, Pileup subtraction using jet areas, Phys. Lett. B 659 (2008) 119, http://dx.doi.org/10.1016/j.physletb.2007.09.077, arXiv:0707.1378.

[54] CMS Collaboration, Performance of CMS muon reconstruction in pp collision events at $\sqrt{s} = 7$ TeV, J. Instrum. (2012) P10002, http://dx.doi.org/10.1088/1748-0221/7/10/P10002, arXiv:1206.4071.

[55] CMS Collaboration, Performance of electron reconstruction and selection with the CMS detector in proton–proton collisions at $\sqrt{s} = 8$ TeV, J. Instrum. 10 (2015) P06005, http://dx.doi.org/10.1088/1748-0221/10/06/P06005, arXiv:1502.02701.

[56] D.-C. Dai, G. Starkman, D. Stojkovic, C. Issever, E. Rizvi, J. Tseng, BlackMax: a black-hole event generator with rotation, recoil, split branes, and brane tension, Phys. Rev. D 77 (2008) 076007, http://dx.doi.org/10.1103/PhysRevD.77.076007, arXiv:0711.3012.

[57] J.A. Frost, J.R. Gaunt, M.O.P. Sampaio, M. Casals, S.R. Dolan, M.A. Parker, B.R. Webber, Phenomenology of production and decay of spinning extra-dimensional black holes at hadron colliders, J. High Energy Phys. 10 (2009) 014, http://dx.doi.org/10.1088/1126-6708/2009/10/014, arXiv:0904.0979.

[58] T. Sjöstrand, S. Ask, J.R. Christiansen, R. Corke, N. Desai, P. Ilten, S. Mrenna, S. Prestel, C.O. Rasmussen, P.Z. Skands, An introduction to PYTHIA 8.2, Comput. Phys. Commun. 191 (2015) 159, http://dx.doi.org/10.1016/j.cpc.2015.01.024, arXiv:1410.3012.

[59] CMS Collaboration, Event generator tunes obtained from underlying event and multiparton scattering measurements, Eur. Phys. J. C 76 (2016) 155, http://dx.doi.org/10.1140/epjc/s10052-016-3988-x, arXiv:1512.00815.

[60] H. Yoshino, V.S. Rychkov, Improved analysis of black hole formation in high-energy particle collisions, Phys. Rev. D 71 (2005) 104028, http://dx.doi.org/10.1103/PhysRevD.71.104028, hep-th/0503171, Erratum: http://dx.doi.org/10.1103/PhysRevD.77.089905.

[61] A.D. Martin, W.J. Stirling, R.S. Thorne, G. Watt, Parton distributions for the LHC, Eur. Phys. J. C 63 (2009) 189, http://dx.doi.org/10.1140/epjc/s10052-009-1072-5, arXiv:0901.0002.

[62] A.D. Martin, W.J. Stirling, R.S. Thorne, G. Watt, Heavy-quark mass dependence in global PDF analyses and 3- and 4-flavour parton distributions, Eur. Phys. J. C 70 (2010) 51, http://dx.doi.org/10.1140/epjc/s10052-010-1462-8, arXiv:1007.2624.

[63] R.D. Ball, et al., NNPDF, Parton distributions for the LHC Run II, J. High Energy Phys. 04 (2015) 040, http://dx.doi.org/10.1007/JHEP04(2015)040, arXiv:1410.8849.

[64] L.A. Harland-Lang, A.D. Martin, P. Motylinski, R.S. Thorne, Parton distributions in the LHC era: MMHT 2014 PDFs, Eur. Phys. J. C 75 (2015) 204, http://dx.doi.org/10.1140/epjc/s10052-015-3397-6, arXiv:1412.3989.

[65] V.N. Ivanchenko, GEANT4, GEANT4 toolkit for simulation of HEP experiments, Nucl. Instrum. Methods A 502 (2003) 666, http://dx.doi.org/10.1016/S0168-9002(03)00538-2.

[66] Douglas Orbaker (on behalf of the CMS Collaboration), Fast simulation of the CMS detector, J. Phys. Conf. Ser. 219 (2010) 032053, http://dx.doi.org/10.1088/1742-6596/219/3/032053.

[67] J. Alwall, R. Frederix, S. Frixione, V. Hirschi, F. Maltoni, O. Mattelaer, H.S. Shao, T. Stelzer, P. Torrielli, M. Zaro, The automated computation of tree-level and next-to-leading order differential cross sections, and their matching to parton shower simulations, J. High Energy Phys. 07 (2014) 079, http://dx.doi.org/10.1007/JHEP07(2014)079, arXiv:1405.0301.

[68] T. Aaltonen, et al., CDF, Search for new particles decaying into dijets in proton-antiproton collisions at $\sqrt{s} = 1.96$ TeV, Phys. Rev. D 79 (2009) 112002, http://dx.doi.org/10.1103/PhysRevD.79.112002, arXiv:0812.4036.

[69] CMS Collaboration, Search for narrow resonances decaying to dijets in proton–proton collisions at $\sqrt{s} = 13$ TeV, Phys. Rev. Lett. 116 (2016) 071801, http://dx.doi.org/10.1103/PhysRevLett.116.071801, arXiv:1512.01224.

[70] CMS Collaboration, Search for resonances and quantum black holes using dijet mass spectra in proton–proton collisions at $\sqrt{s} = 8$ TeV, Phys. Rev. D 91 (2015) 052009, http://dx.doi.org/10.1103/PhysRevD.91.052009, arXiv:1501.04198.

[71] J. Pumplin, D.R. Stump, J. Huston, H.L. Lai, P.M. Nadolsky, W.K. Tung, New generation of parton distributions with uncertainties from global QCD analysis, J. High Energy Phys. 07 (2002) 012, http://dx.doi.org/10.1088/1126-6708/2002/07/012, arXiv:hep-ph/0201195.

[72] H.-L. Lai, M. Guzzi, J. Huston, Z. Li, P.M. Nadolsky, J. Pumplin, C.P. Yuan, New parton distributions for collider physics, Phys. Rev. D 82 (2010) 074024, http://dx.doi.org/10.1103/PhysRevD.82.074024, arXiv:1007.2241.

[73] S. Alekhin, et al., The PDF4LHC Working Group Interim Report, arXiv:1101.0536, 2011.

[74] M. Botje, J. Butterworth, A. Cooper-Sarkar, A. de Roeck, J. Feltesse, S. Forte, A. Glazov, J. Huston, R. McNulty, T. Sjöstrand, R.S. Thorne, The PDF4LHC Working Group Interim Recommendations, arXiv:1101.0538, 2011.

[75] CMS Collaboration, CMS Luminosity Measurement for the 2015 Data Taking Period, CMS Physics Analysis Summary CMS-PAS-LUM-15-001. CERN, Geneva, 2016, https://cds.cern.ch/record/2138682.

[76] T. Junk, Confidence level computation for combining searches with small statistics, Nucl. Instrum. Methods A 434 (1999) 435, http://dx.doi.org/10.1016/S0168-9002(99)00498-2, arXiv:hep-ex/9902006.

[77] A.L. Read, Presentation of search results: the CL_s technique, J. Phys. G 28 (2002) 26934, http://dx.doi.org/10.1088/0954-3899/28/10/313.
[78] ATLAS, CMS Collaborations, Procedure for the LHC Higgs boson search combination in Summer 2011, ATLAS-PHYS-PUB-2011-011, CMS Note 2011/005, 2011, https://cds.cern.ch/record/1379837.
[79] R.D. Cousins, J.T. Linnemann, J. Tucker, Evaluation of three methods for calculating statistical significance when incorporating a systematic uncertainty into a test of the background-only hypothesis for a poisson process, Nucl. Instrum. Methods A 595 (2008) 480, http://dx.doi.org/10.1016/j.nima.2008.07.086.

The CMS Collaboration

A.M. Sirunyan, A. Tumasyan

Yerevan Physics Institute, Yerevan, Armenia

W. Adam, E. Asilar, T. Bergauer, J. Brandstetter, E. Brondolin, M. Dragicevic, J. Erö, M. Flechl, M. Friedl, R. Frühwirth [1], V.M. Ghete, C. Hartl, N. Hörmann, J. Hrubec, M. Jeitler [1], A. König, I. Krätschmer, D. Liko, T. Matsushita, I. Mikulec, D. Rabady, N. Rad, B. Rahbaran, H. Rohringer, J. Schieck [1], J. Strauss, W. Waltenberger, C.-E. Wulz [1]

Institut für Hochenergiephysik, Wien, Austria

O. Dvornikov, V. Makarenko, V. Mossolov, J. Suarez Gonzalez, V. Zykunov

Institute for Nuclear Problems, Minsk, Belarus

N. Shumeiko

National Centre for Particle and High Energy Physics, Minsk, Belarus

S. Alderweireldt, E.A. De Wolf, X. Janssen, J. Lauwers, M. Van De Klundert, H. Van Haevermaet, P. Van Mechelen, N. Van Remortel, A. Van Spilbeeck

Universiteit Antwerpen, Antwerpen, Belgium

S. Abu Zeid, F. Blekman, J. D'Hondt, N. Daci, I. De Bruyn, K. Deroover, S. Lowette, S. Moortgat, L. Moreels, A. Olbrechts, Q. Python, K. Skovpen, S. Tavernier, W. Van Doninck, P. Van Mulders, I. Van Parijs

Vrije Universiteit Brussel, Brussel, Belgium

H. Brun, B. Clerbaux, G. De Lentdecker, H. Delannoy, G. Fasanella, L. Favart, R. Goldouzian, A. Grebenyuk, G. Karapostoli, T. Lenzi, A. Léonard, J. Luetic, T. Maerschalk, A. Marinov, A. Randle-conde, T. Seva, C. Vander Velde, P. Vanlaer, D. Vannerom, R. Yonamine, F. Zenoni, F. Zhang [2]

Université Libre de Bruxelles, Bruxelles, Belgium

A. Cimmino, T. Cornelis, D. Dobur, A. Fagot, M. Gul, I. Khvastunov, D. Poyraz, S. Salva, R. Schöfbeck, M. Tytgat, W. Van Driessche, E. Yazgan, N. Zaganidis

Ghent University, Ghent, Belgium

H. Bakhshiansohi, C. Beluffi [3], O. Bondu, S. Brochet, G. Bruno, A. Caudron, S. De Visscher, C. Delaere, M. Delcourt, B. Francois, A. Giammanco, A. Jafari, M. Komm, G. Krintiras, V. Lemaitre, A. Magitteri, A. Mertens, M. Musich, K. Piotrzkowski, L. Quertenmont, M. Selvaggi, M. Vidal Marono, S. Wertz

Université Catholique de Louvain, Louvain-la-Neuve, Belgium

N. Beliy

Université de Mons, Mons, Belgium

W.L. Aldá Júnior, F.L. Alves, G.A. Alves, L. Brito, C. Hensel, A. Moraes, M.E. Pol, P. Rebello Teles

Centro Brasileiro de Pesquisas Fisicas, Rio de Janeiro, Brazil

E. Belchior Batista Das Chagas, W. Carvalho, J. Chinellato [4], A. Custódio, E.M. Da Costa, G.G. Da Silveira [5], D. De Jesus Damiao, C. De Oliveira Martins, S. Fonseca De Souza, L.M. Huertas Guativa, H. Malbouisson,

D. Matos Figueiredo, C. Mora Herrera, L. Mundim, H. Nogima, W.L. Prado Da Silva, A. Santoro, A. Sznajder, E.J. Tonelli Manganote [4], F. Torres Da Silva De Araujo, A. Vilela Pereira

Universidade do Estado do Rio de Janeiro, Rio de Janeiro, Brazil

S. Ahuja [a], C.A. Bernardes [a], S. Dogra [a], T.R. Fernandez Perez Tomei [a], E.M. Gregores [b], P.G. Mercadante [b], C.S. Moon [a], S.F. Novaes [a], Sandra S. Padula [a], D. Romero Abad [b], J.C. Ruiz Vargas [a]

[a] *Universidade Estadual Paulista, São Paulo, Brazil*
[b] *Universidade Federal do ABC, São Paulo, Brazil*

A. Aleksandrov, R. Hadjiiska, P. Iaydjiev, M. Rodozov, S. Stoykova, G. Sultanov, M. Vutova

Institute for Nuclear Research and Nuclear Energy, Sofia, Bulgaria

A. Dimitrov, I. Glushkov, L. Litov, B. Pavlov, P. Petkov

University of Sofia, Sofia, Bulgaria

W. Fang [6]

Beihang University, Beijing, China

M. Ahmad, J.G. Bian, G.M. Chen, H.S. Chen, M. Chen, Y. Chen [7], T. Cheng, C.H. Jiang, D. Leggat, Z. Liu, F. Romeo, M. Ruan, S.M. Shaheen, A. Spiezia, J. Tao, C. Wang, Z. Wang, H. Zhang, J. Zhao

Institute of High Energy Physics, Beijing, China

Y. Ban, G. Chen, Q. Li, S. Liu, Y. Mao, S.J. Qian, D. Wang, Z. Xu

State Key Laboratory of Nuclear Physics and Technology, Peking University, Beijing, China

C. Avila, A. Cabrera, L.F. Chaparro Sierra, C. Florez, J.P. Gomez, C.F. González Hernández, J.D. Ruiz Alvarez, J.C. Sanabria

Universidad de Los Andes, Bogota, Colombia

N. Godinovic, D. Lelas, I. Puljak, P.M. Ribeiro Cipriano, T. Sculac

University of Split, Faculty of Electrical Engineering, Mechanical Engineering and Naval Architecture, Split, Croatia

Z. Antunovic, M. Kovac

University of Split, Faculty of Science, Split, Croatia

V. Brigljevic, D. Ferencek, K. Kadija, B. Mesic, T. Susa

Institute Rudjer Boskovic, Zagreb, Croatia

A. Attikis, G. Mavromanolakis, J. Mousa, C. Nicolaou, F. Ptochos, P.A. Razis, H. Rykaczewski, D. Tsiakkouri

University of Cyprus, Nicosia, Cyprus

M. Finger [8], M. Finger Jr. [8]

Charles University, Prague, Czech Republic

E. Carrera Jarrin

Universidad San Francisco de Quito, Quito, Ecuador

Y. Assran [9,10], T. Elkafrawy [11], A. Mahrous [12]

Academy of Scientific Research and Technology of the Arab Republic of Egypt, Egyptian Network of High Energy Physics, Cairo, Egypt

M. Kadastik, L. Perrini, M. Raidal, A. Tiko, C. Veelken

National Institute of Chemical Physics and Biophysics, Tallinn, Estonia

P. Eerola, J. Pekkanen, M. Voutilainen

Department of Physics, University of Helsinki, Helsinki, Finland

J. Härkönen, T. Järvinen, V. Karimäki, R. Kinnunen, T. Lampén, K. Lassila-Perini, S. Lehti, T. Lindén, P. Luukka, J. Tuominiemi, E. Tuovinen, L. Wendland

Helsinki Institute of Physics, Helsinki, Finland

J. Talvitie, T. Tuuva

Lappeenranta University of Technology, Lappeenranta, Finland

M. Besancon, F. Couderc, M. Dejardin, D. Denegri, B. Fabbro, J.L. Faure, C. Favaro, F. Ferri, S. Ganjour, S. Ghosh, A. Givernaud, P. Gras, G. Hamel de Monchenault, P. Jarry, I. Kucher, E. Locci, M. Machet, J. Malcles, J. Rander, A. Rosowsky, M. Titov

IRFU, CEA, Université Paris-Saclay, Gif-sur-Yvette, France

A. Abdulsalam, I. Antropov, S. Baffioni, F. Beaudette, P. Busson, L. Cadamuro, E. Chapon, C. Charlot, O. Davignon, R. Granier de Cassagnac, M. Jo, S. Lisniak, P. Miné, M. Nguyen, C. Ochando, G. Ortona, P. Paganini, P. Pigard, S. Regnard, R. Salerno, Y. Sirois, A.G. Stahl Leiton, T. Strebler, Y. Yilmaz, A. Zabi, A. Zghiche

Laboratoire Leprince-Ringuet, Ecole polytechnique, CNRS/IN2P3, Université Paris-Saclay, Palaiseau, France

J.-L. Agram [13], J. Andrea, A. Aubin, D. Bloch, J.-M. Brom, M. Buttignol, E.C. Chabert, N. Chanon, C. Collard, E. Conte [13], X. Coubez, J.-C. Fontaine [13], D. Gelé, U. Goerlach, A.-C. Le Bihan, P. Van Hove

Université de Strasbourg, CNRS, IPHC UMR 7178, F-67000 Strasbourg, France

S. Gadrat

Centre de Calcul de l'Institut National de Physique Nucleaire et de Physique des Particules, CNRS/IN2P3, Villeurbanne, France

S. Beauceron, C. Bernet, G. Boudoul, C.A. Carrillo Montoya, R. Chierici, D. Contardo, B. Courbon, P. Depasse, H. El Mamouni, J. Fay, S. Gascon, M. Gouzevitch, G. Grenier, B. Ille, F. Lagarde, I.B. Laktineh, M. Lethuillier, L. Mirabito, A.L. Pequegnot, S. Perries, A. Popov [14], D. Sabes, V. Sordini, M. Vander Donckt, P. Verdier, S. Viret

Université de Lyon, Université Claude Bernard Lyon 1, CNRS-IN2P3, Institut de Physique Nucléaire de Lyon, Villeurbanne, France

T. Toriashvili [15]

Georgian Technical University, Tbilisi, Georgia

Z. Tsamalaidze [8]

Tbilisi State University, Tbilisi, Georgia

C. Autermann, S. Beranek, L. Feld, M.K. Kiesel, K. Klein, M. Lipinski, M. Preuten, C. Schomakers, J. Schulz, T. Verlage

RWTH Aachen University, I. Physikalisches Institut, Aachen, Germany

A. Albert, M. Brodski, E. Dietz-Laursonn, D. Duchardt, M. Endres, M. Erdmann, S. Erdweg, T. Esch, R. Fischer, A. Güth, M. Hamer, T. Hebbeker, C. Heidemann, K. Hoepfner, S. Knutzen, M. Merschmeyer, A. Meyer, P. Millet, S. Mukherjee, M. Olschewski, K. Padeken, T. Pook, M. Radziej, H. Reithler, M. Rieger, F. Scheuch, L. Sonnenschein, D. Teyssier, S. Thüer

RWTH Aachen University, III. Physikalisches Institut A, Aachen, Germany

V. Cherepanov, G. Flügge, B. Kargoll, T. Kress, A. Künsken, J. Lingemann, T. Müller, A. Nehrkorn, A. Nowack, C. Pistone, O. Pooth, A. Stahl [16]

RWTH Aachen University, III. Physikalisches Institut B, Aachen, Germany

M. Aldaya Martin, T. Arndt, C. Asawatangtrakuldee, K. Beernaert, O. Behnke, U. Behrens, A.A. Bin Anuar, K. Borras [17], A. Campbell, P. Connor, C. Contreras-Campana, F. Costanza, C. Diez Pardos, G. Dolinska, G. Eckerlin, D. Eckstein, T. Eichhorn, E. Eren, E. Gallo [18], J. Garay Garcia, A. Geiser, A. Gizhko, J.M. Grados Luyando, A. Grohsjean, P. Gunnellini, A. Harb, J. Hauk, M. Hempel [19], H. Jung, A. Kalogeropoulos, O. Karacheban [19], M. Kasemann, J. Keaveney, C. Kleinwort, I. Korol, D. Krücker, W. Lange, A. Lelek, T. Lenz, J. Leonard, K. Lipka, A. Lobanov, W. Lohmann [19], R. Mankel, I.-A. Melzer-Pellmann, A.B. Meyer, G. Mittag, J. Mnich, A. Mussgiller, D. Pitzl, R. Placakyte, A. Raspereza, B. Roland, M.Ö. Sahin, P. Saxena, T. Schoerner-Sadenius, S. Spannagel, N. Stefaniuk, G.P. Van Onsem, R. Walsh, C. Wissing

Deutsches Elektronen-Synchrotron, Hamburg, Germany

V. Blobel, M. Centis Vignali, A.R. Draeger, T. Dreyer, E. Garutti, D. Gonzalez, J. Haller, M. Hoffmann, A. Junkes, R. Klanner, R. Kogler, N. Kovalchuk, T. Lapsien, I. Marchesini, D. Marconi, M. Meyer, M. Niedziela, D. Nowatschin, F. Pantaleo [16], T. Peiffer, A. Perieanu, C. Scharf, P. Schleper, A. Schmidt, S. Schumann, J. Schwandt, H. Stadie, G. Steinbrück, F.M. Stober, M. Stöver, H. Tholen, D. Troendle, E. Usai, L. Vanelderen, A. Vanhoefer, B. Vormwald

University of Hamburg, Hamburg, Germany

M. Akbiyik, C. Barth, S. Baur, C. Baus, J. Berger, E. Butz, R. Caspart, T. Chwalek, F. Colombo, W. De Boer, A. Dierlamm, S. Fink, B. Freund, R. Friese, M. Giffels, A. Gilbert, P. Goldenzweig, D. Haitz, F. Hartmann [16], S.M. Heindl, U. Husemann, I. Katkov [14], S. Kudella, H. Mildner, M.U. Mozer, Th. Müller, M. Plagge, G. Quast, K. Rabbertz, S. Röcker, F. Roscher, M. Schröder, I. Shvetsov, G. Sieber, H.J. Simonis, R. Ulrich, S. Wayand, M. Weber, T. Weiler, S. Williamson, C. Wöhrmann, R. Wolf

Institut für Experimentelle Kernphysik, Karlsruhe, Germany

G. Anagnostou, G. Daskalakis, T. Geralis, V.A. Giakoumopoulou, A. Kyriakis, D. Loukas, I. Topsis-Giotis

Institute of Nuclear and Particle Physics (INPP), NCSR Demokritos, Aghia Paraskevi, Greece

S. Kesisoglou, A. Panagiotou, N. Saoulidou, E. Tziaferi

National and Kapodistrian University of Athens, Athens, Greece

I. Evangelou, G. Flouris, C. Foudas, P. Kokkas, N. Loukas, N. Manthos, I. Papadopoulos, E. Paradas

University of Ioánnina, Ioánnina, Greece

N. Filipovic, G. Pasztor

MTA-ELTE Lendület CMS Particle and Nuclear Physics Group, Eötvös Loránd University, Budapest, Hungary

G. Bencze, C. Hajdu, D. Horvath [20], F. Sikler, V. Veszpremi, G. Vesztergombi [21], A.J. Zsigmond

Wigner Research Centre for Physics, Budapest, Hungary

N. Beni, S. Czellar, J. Karancsi [22], A. Makovec, J. Molnar, Z. Szillasi

Institute of Nuclear Research ATOMKI, Debrecen, Hungary

M. Bartók [21], P. Raics, Z.L. Trocsanyi, B. Ujvari

Institute of Physics, University of Debrecen, Debrecen, Hungary

J.R. Komaragiri

Indian Institute of Science (IISc), Bangalore, India

S. Bahinipati [23], S. Bhowmik [24], S. Choudhury [25], P. Mal, K. Mandal, A. Nayak [26], D.K. Sahoo [23], N. Sahoo, S.K. Swain

National Institute of Science Education and Research, Bhubaneswar, India

S. Bansal, S.B. Beri, V. Bhatnagar, R. Chawla, U. Bhawandeep, A.K. Kalsi, A. Kaur, M. Kaur, R. Kumar, P. Kumari, A. Mehta, M. Mittal, J.B. Singh, G. Walia

Panjab University, Chandigarh, India

Ashok Kumar, A. Bhardwaj, B.C. Choudhary, R.B. Garg, S. Keshri, S. Malhotra, M. Naimuddin, K. Ranjan, R. Sharma, V. Sharma

University of Delhi, Delhi, India

R. Bhattacharya, S. Bhattacharya, K. Chatterjee, S. Dey, S. Dutt, S. Dutta, S. Ghosh, N. Majumdar, A. Modak, K. Mondal, S. Mukhopadhyay, S. Nandan, A. Purohit, A. Roy, D. Roy, S. Roy Chowdhury, S. Sarkar, M. Sharan, S. Thakur

Saha Institute of Nuclear Physics, Kolkata, India

P.K. Behera

Indian Institute of Technology Madras, Madras, India

R. Chudasama, D. Dutta, V. Jha, V. Kumar, A.K. Mohanty [16], P.K. Netrakanti, L.M. Pant, P. Shukla, A. Topkar

Bhabha Atomic Research Centre, Mumbai, India

T. Aziz, S. Dugad, G. Kole, B. Mahakud, S. Mitra, G.B. Mohanty, B. Parida, N. Sur, B. Sutar

Tata Institute of Fundamental Research-A, Mumbai, India

S. Banerjee, R.K. Dewanjee, S. Ganguly, M. Guchait, Sa. Jain, S. Kumar, M. Maity [24], G. Majumder, K. Mazumdar, T. Sarkar [24], N. Wickramage [27]

Tata Institute of Fundamental Research-B, Mumbai, India

S. Chauhan, S. Dube, V. Hegde, A. Kapoor, K. Kothekar, S. Pandey, A. Rane, S. Sharma

Indian Institute of Science Education and Research (IISER), Pune, India

S. Chenarani [28], E. Eskandari Tadavani, S.M. Etesami [28], M. Khakzad, M. Mohammadi Najafabadi, M. Naseri, S. Paktinat Mehdiabadi [29], F. Rezaei Hosseinabadi, B. Safarzadeh [30], M. Zeinali

Institute for Research in Fundamental Sciences (IPM), Tehran, Iran

M. Felcini, M. Grunewald

University College Dublin, Dublin, Ireland

M. Abbrescia [a,b], C. Calabria [a,b], C. Caputo [a,b], A. Colaleo [a], D. Creanza [a,c], L. Cristella [a,b], N. De Filippis [a,c], M. De Palma [a,b], L. Fiore [a], G. Iaselli [a,c], G. Maggi [a,c], M. Maggi [a], G. Miniello [a,b], S. My [a,b], S. Nuzzo [a,b], A. Pompili [a,b], G. Pugliese [a,c], R. Radogna [a,b], A. Ranieri [a], G. Selvaggi [a,b], A. Sharma [a], L. Silvestris [a,16], R. Venditti [a,b], P. Verwilligen [a]

[a] *INFN Sezione di Bari, Bari, Italy*
[b] *Università di Bari, Bari, Italy*
[c] *Politecnico di Bari, Bari, Italy*

G. Abbiendi [a], C. Battilana, D. Bonacorsi [a,b], S. Braibant-Giacomelli [a,b], L. Brigliadori [a,b], R. Campanini [a,b], P. Capiluppi [a,b], A. Castro [a,b], F.R. Cavallo [a], S.S. Chhibra [a,b], G. Codispoti [a,b], M. Cuffiani [a,b], G.M. Dallavalle [a], F. Fabbri [a], A. Fanfani [a,b], D. Fasanella [a,b], P. Giacomelli [a], C. Grandi [a], L. Guiducci [a,b],

S. Marcellini [a], G. Masetti [a], A. Montanari [a], F.L. Navarria [a,b], A. Perrotta [a], A.M. Rossi [a,b], T. Rovelli [a,b], G.P. Siroli [a,b], N. Tosi [a,b,16]

[a] INFN Sezione di Bologna, Bologna, Italy
[b] Università di Bologna, Bologna, Italy

S. Albergo [a,b], S. Costa [a,b], A. Di Mattia [a], F. Giordano [a,b], R. Potenza [a,b], A. Tricomi [a,b], C. Tuve [a,b]

[a] INFN Sezione di Catania, Catania, Italy
[b] Università di Catania, Catania, Italy

G. Barbagli [a], V. Ciulli [a,b], C. Civinini [a], R. D'Alessandro [a,b], E. Focardi [a,b], P. Lenzi [a,b], M. Meschini [a], S. Paoletti [a], L. Russo [a,31], G. Sguazzoni [a], D. Strom [a], L. Viliani [a,b,16]

[a] INFN Sezione di Firenze, Firenze, Italy
[b] Università di Firenze, Firenze, Italy

L. Benussi, S. Bianco, F. Fabbri, D. Piccolo, F. Primavera [16]

INFN Laboratori Nazionali di Frascati, Frascati, Italy

V. Calvelli [a,b], F. Ferro [a], M.R. Monge [a,b], E. Robutti [a], S. Tosi [a,b]

[a] INFN Sezione di Genova, Genova, Italy
[b] Università di Genova, Genova, Italy

L. Brianza [a,b,16], F. Brivio [a,b], V. Ciriolo, M.E. Dinardo [a,b], S. Fiorendi [a,b,16], S. Gennai [a], A. Ghezzi [a,b], P. Govoni [a,b], M. Malberti [a,b], S. Malvezzi [a], R.A. Manzoni [a,b], D. Menasce [a], L. Moroni [a], M. Paganoni [a,b], D. Pedrini [a], S. Pigazzini [a,b], S. Ragazzi [a,b], T. Tabarelli de Fatis [a,b]

[a] INFN Sezione di Milano-Bicocca, Milano, Italy
[b] Università di Milano-Bicocca, Milano, Italy

S. Buontempo [a], N. Cavallo [a,c], G. De Nardo, S. Di Guida [a,d,16], F. Fabozzi [a,c], F. Fienga [a,b], A.O.M. Iorio [a,b], L. Lista [a], S. Meola [a,d,16], P. Paolucci [a,16], C. Sciacca [a,b], F. Thyssen [a]

[a] INFN Sezione di Napoli, Napoli, Italy
[b] Università di Napoli 'Federico II', Napoli, Italy
[c] Università della Basilicata, Potenza, Italy
[d] Università G. Marconi, Roma, Italy

P. Azzi [a,16], N. Bacchetta [a], L. Benato [a,b], D. Bisello [a,b], A. Boletti [a,b], R. Carlin [a,b], A. Carvalho Antunes De Oliveira [a,b], P. Checchia [a], M. Dall'Osso [a,b], P. De Castro Manzano [a], T. Dorigo [a], U. Dosselli [a], F. Gasparini [a,b], U. Gasparini [a,b], A. Gozzelino [a], S. Lacaprara [a], M. Margoni [a,b], A.T. Meneguzzo [a,b], J. Pazzini [a,b], N. Pozzobon [a,b], P. Ronchese [a,b], F. Simonetto [a,b], E. Torassa [a], M. Zanetti [a,b], P. Zotto [a,b], G. Zumerle [a,b]

[a] INFN Sezione di Padova, Padova, Italy
[b] Università di Padova, Padova, Italy
[c] Università di Trento, Trento, Italy

A. Braghieri [a], F. Fallavollita [a,b], A. Magnani [a,b], P. Montagna [a,b], S.P. Ratti [a,b], V. Re [a], C. Riccardi [a,b], P. Salvini [a], I. Vai [a,b], P. Vitulo [a,b]

[a] INFN Sezione di Pavia, Pavia, Italy
[b] Università di Pavia, Pavia, Italy

L. Alunni Solestizi [a,b], G.M. Bilei [a], D. Ciangottini [a,b], L. Fanò [a,b], P. Lariccia [a,b], R. Leonardi [a,b], G. Mantovani [a,b], M. Menichelli [a], A. Saha [a], A. Santocchia [a,b]

[a] INFN Sezione di Perugia, Perugia, Italy
[b] Università di Perugia, Perugia, Italy

K. Androsov [a,31], P. Azzurri [a,16], G. Bagliesi [a], J. Bernardini [a], T. Boccali [a], R. Castaldi [a], M.A. Ciocci [a,31], R. Dell'Orso [a], S. Donato [a,c], G. Fedi, A. Giassi [a], M.T. Grippo [a,31], F. Ligabue [a,c], T. Lomtadze [a], L. Martini [a,b],

A. Messineo [a,b], F. Palla [a], A. Rizzi [a,b], A. Savoy-Navarro [a,32], P. Spagnolo [a], R. Tenchini [a], G. Tonelli [a,b], A. Venturi [a], P.G. Verdini [a]

[a] INFN Sezione di Pisa, Pisa, Italy
[b] Università di Pisa, Pisa, Italy
[c] Scuola Normale Superiore di Pisa, Pisa, Italy

L. Barone [a,b], F. Cavallari [a], M. Cipriani [a,b], D. Del Re [a,b,16], M. Diemoz [a], S. Gelli [a,b], E. Longo [a,b], F. Margaroli [a,b], B. Marzocchi [a,b], P. Meridiani [a], G. Organtini [a,b], R. Paramatti [a], F. Preiato [a,b], S. Rahatlou [a,b], C. Rovelli [a], F. Santanastasio [a,b]

[a] INFN Sezione di Roma, Rome, Italy
[b] Sapienza Università di Roma, Rome, Italy

N. Amapane [a,b], R. Arcidiacono [a,c,16], S. Argiro [a,b], M. Arneodo [a,c], N. Bartosik [a], R. Bellan [a,b], C. Biino [a], N. Cartiglia [a], F. Cenna [a,b], M. Costa [a,b], R. Covarelli [a,b], A. Degano [a,b], N. Demaria [a], L. Finco [a,b], B. Kiani [a,b], C. Mariotti [a], S. Maselli [a], E. Migliore [a,b], V. Monaco [a,b], E. Monteil [a,b], M. Monteno [a], M.M. Obertino [a,b], L. Pacher [a,b], N. Pastrone [a], M. Pelliccioni [a], G.L. Pinna Angioni [a,b], F. Ravera [a,b], A. Romero [a,b], M. Ruspa [a,c], R. Sacchi [a,b], K. Shchelina [a,b], V. Sola [a], A. Solano [a,b], A. Staiano [a], P. Traczyk [a,b]

[a] INFN Sezione di Torino, Torino, Italy
[b] Università di Torino, Torino, Italy
[c] Università del Piemonte Orientale, Novara, Italy

S. Belforte [a], M. Casarsa [a], F. Cossutti [a], G. Della Ricca [a,b], A. Zanetti [a]

[a] INFN Sezione di Trieste, Trieste, Italy
[b] Università di Trieste, Trieste, Italy

D.H. Kim, G.N. Kim, M.S. Kim, S. Lee, S.W. Lee, Y.D. Oh, S. Sekmen, D.C. Son, Y.C. Yang

Kyungpook National University, Daegu, Republic of Korea

A. Lee

Chonbuk National University, Jeonju, Republic of Korea

H. Kim

Chonnam National University, Institute for Universe and Elementary Particles, Kwangju, Republic of Korea

J.A. Brochero Cifuentes, T.J. Kim

Hanyang University, Seoul, Republic of Korea

S. Cho, S. Choi, Y. Go, D. Gyun, S. Ha, B. Hong, Y. Jo, Y. Kim, K. Lee, K.S. Lee, S. Lee, J. Lim, S.K. Park, Y. Roh

Korea University, Seoul, Republic of Korea

J. Almond, J. Kim, H. Lee, S.B. Oh, B.C. Radburn-Smith, S.h. Seo, U.K. Yang, H.D. Yoo, G.B. Yu

Seoul National University, Seoul, Republic of Korea

M. Choi, H. Kim, J.H. Kim, J.S.H. Lee, I.C. Park, G. Ryu, M.S. Ryu

University of Seoul, Seoul, Republic of Korea

Y. Choi, J. Goh, C. Hwang, J. Lee, I. Yu

Sungkyunkwan University, Suwon, Republic of Korea

V. Dudenas, A. Juodagalvis, J. Vaitkus

Vilnius University, Vilnius, Lithuania

I. Ahmed, Z.A. Ibrahim, M.A.B. Md Ali [33], F. Mohamad Idris [34], W.A.T. Wan Abdullah, M.N. Yusli, Z. Zolkapli

National Centre for Particle Physics, Universiti Malaya, Kuala Lumpur, Malaysia

H. Castilla-Valdez, E. De La Cruz-Burelo, I. Heredia-De La Cruz [35], A. Hernandez-Almada, R. Lopez-Fernandez, R. Magaña Villalba, J. Mejia Guisao, A. Sanchez-Hernandez

Centro de Investigacion y de Estudios Avanzados del IPN, Mexico City, Mexico

S. Carrillo Moreno, C. Oropeza Barrera, F. Vazquez Valencia

Universidad Iberoamericana, Mexico City, Mexico

S. Carpinteyro, I. Pedraza, H.A. Salazar Ibarguen, C. Uribe Estrada

Benemerita Universidad Autonoma de Puebla, Puebla, Mexico

A. Morelos Pineda

Universidad Autónoma de San Luis Potosí, San Luis Potosí, Mexico

D. Krofcheck

University of Auckland, Auckland, New Zealand

P.H. Butler

University of Canterbury, Christchurch, New Zealand

A. Ahmad, M. Ahmad, Q. Hassan, H.R. Hoorani, W.A. Khan, A. Saddique, M.A. Shah, M. Shoaib, M. Waqas

National Centre for Physics, Quaid-I-Azam University, Islamabad, Pakistan

H. Bialkowska, M. Bluj, B. Boimska, T. Frueboes, M. Górski, M. Kazana, K. Nawrocki, K. Romanowska-Rybinska, M. Szleper, P. Zalewski

National Centre for Nuclear Research, Swierk, Poland

K. Bunkowski, A. Byszuk [36], K. Doroba, A. Kalinowski, M. Konecki, J. Krolikowski, M. Misiura, M. Olszewski, M. Walczak

Institute of Experimental Physics, Faculty of Physics, University of Warsaw, Warsaw, Poland

P. Bargassa, C. Beirão Da Cruz E Silva, B. Calpas, A. Di Francesco, P. Faccioli, P.G. Ferreira Parracho, M. Gallinaro, J. Hollar, N. Leonardo, L. Lloret Iglesias, M.V. Nemallapudi, J. Rodrigues Antunes, J. Seixas, O. Toldaiev, D. Vadruccio, J. Varela

Laboratório de Instrumentação e Física Experimental de Partículas, Lisboa, Portugal

V. Alexakhin, I. Belotelov, P. Bunin, M. Gavrilenko, I. Golutvin, I. Gorbunov, V. Karjavin, A. Lanev, A. Malakhov, V. Matveev [37,38], V. Palichik, V. Perelygin, M. Savina, S. Shmatov, S. Shulha, N. Skatchkov, V. Smirnov, A. Zarubin

Joint Institute for Nuclear Research, Dubna, Russia

L. Chtchipounov, V. Golovtsov, Y. Ivanov, V. Kim [39], E. Kuznetsova [40], V. Murzin, V. Oreshkin, V. Sulimov, A. Vorobyev

Petersburg Nuclear Physics Institute, Gatchina (St. Petersburg), Russia

Yu. Andreev, A. Dermenev, S. Gninenko, N. Golubev, A. Karneyeu, M. Kirsanov, N. Krasnikov, A. Pashenkov, D. Tlisov, A. Toropin

Institute for Nuclear Research, Moscow, Russia

V. Epshteyn, V. Gavrilov, N. Lychkovskaya, V. Popov, I. Pozdnyakov, G. Safronov, A. Spiridonov, M. Toms, E. Vlasov, A. Zhokin

Institute for Theoretical and Experimental Physics, Moscow, Russia

T. Aushev, A. Bylinkin [38]

Moscow Institute of Physics and Technology, Moscow, Russia

M. Chadeeva [41], O. Markin, E. Tarkovskii

National Research Nuclear University 'Moscow Engineering Physics Institute' (MEPhI), Moscow, Russia

V. Andreev, M. Azarkin [38], I. Dremin [38], M. Kirakosyan, A. Leonidov [38], A. Terkulov

P.N. Lebedev Physical Institute, Moscow, Russia

A. Baskakov, A. Belyaev, E. Boos, V. Bunichev, M. Dubinin [42], L. Dudko, A. Ershov, A. Gribushin, V. Klyukhin, O. Kodolova, I. Lokhtin, I. Miagkov, S. Obraztsov, S. Petrushanko, V. Savrin

Skobeltsyn Institute of Nuclear Physics, Lomonosov Moscow State University, Moscow, Russia

V. Blinov [43], Y. Skovpen [43], D. Shtol [43]

Novosibirsk State University (NSU), Novosibirsk, Russia

I. Azhgirey, I. Bayshev, S. Bitioukov, D. Elumakhov, V. Kachanov, A. Kalinin, D. Konstantinov, V. Krychkine, V. Petrov, R. Ryutin, A. Sobol, S. Troshin, N. Tyurin, A. Uzunian, A. Volkov

State Research Center of Russian Federation, Institute for High Energy Physics, Protvino, Russia

P. Adzic [44], P. Cirkovic, D. Devetak, M. Dordevic, J. Milosevic, V. Rekovic

University of Belgrade, Faculty of Physics and Vinca Institute of Nuclear Sciences, Belgrade, Serbia

J. Alcaraz Maestre, M. Barrio Luna, E. Calvo, M. Cerrada, M. Chamizo Llatas, N. Colino, B. De La Cruz, A. Delgado Peris, A. Escalante Del Valle, C. Fernandez Bedoya, J.P. Fernández Ramos, J. Flix, M.C. Fouz, P. Garcia-Abia, O. Gonzalez Lopez, S. Goy Lopez, J.M. Hernandez, M.I. Josa, E. Navarro De Martino, A. Pérez-Calero Yzquierdo, J. Puerta Pelayo, A. Quintario Olmeda, I. Redondo, L. Romero, M.S. Soares

Centro de Investigaciones Energéticas Medioambientales y Tecnológicas (CIEMAT), Madrid, Spain

J.F. de Trocóniz, M. Missiroli, D. Moran

Universidad Autónoma de Madrid, Madrid, Spain

J. Cuevas, J. Fernandez Menendez, I. Gonzalez Caballero, J.R. González Fernández, E. Palencia Cortezon, S. Sanchez Cruz, I. Suárez Andrés, P. Vischia, J.M. Vizan Garcia

Universidad de Oviedo, Oviedo, Spain

I.J. Cabrillo, A. Calderon, E. Curras, M. Fernandez, J. Garcia-Ferrero, G. Gomez, A. Lopez Virto, J. Marco, C. Martinez Rivero, F. Matorras, J. Piedra Gomez, T. Rodrigo, A. Ruiz-Jimeno, L. Scodellaro, N. Trevisani, I. Vila, R. Vilar Cortabitarte

Instituto de Física de Cantabria (IFCA), CSIC-Universidad de Cantabria, Santander, Spain

D. Abbaneo, E. Auffray, G. Auzinger, P. Baillon, A.H. Ball, D. Barney, P. Bloch, A. Bocci, C. Botta, T. Camporesi, R. Castello, M. Cepeda, G. Cerminara, Y. Chen, D. d'Enterria, A. Dabrowski, V. Daponte, A. David, M. De Gruttola, A. De Roeck, E. Di Marco [45], M. Dobson, B. Dorney, T. du Pree, D. Duggan, M. Dünser, N. Dupont, A. Elliott-Peisert, P. Everaerts, S. Fartoukh, G. Franzoni, J. Fulcher, W. Funk, D. Gigi, K. Gill, M. Girone, F. Glege, D. Gulhan, S. Gundacker, M. Guthoff, P. Harris, J. Hegeman, V. Innocente, P. Janot, J. Kieseler, H. Kirschenmann, V. Knünz, A. Kornmayer [16], M.J. Kortelainen, K. Kousouris,

M. Krammer [1], C. Lange, P. Lecoq, C. Lourenço, M.T. Lucchini, L. Malgeri, M. Mannelli, A. Martelli, F. Meijers, J.A. Merlin, S. Mersi, E. Meschi, P. Milenovic [46], F. Moortgat, S. Morovic, M. Mulders, H. Neugebauer, S. Orfanelli, L. Orsini, L. Pape, E. Perez, M. Peruzzi, A. Petrilli, G. Petrucciani, A. Pfeiffer, M. Pierini, A. Racz, T. Reis, G. Rolandi [47], M. Rovere, H. Sakulin, J.B. Sauvan, C. Schäfer, C. Schwick, M. Seidel, A. Sharma, P. Silva, P. Sphicas [48], J. Steggemann, M. Stoye, Y. Takahashi, M. Tosi, D. Treille, A. Triossi, A. Tsirou, V. Veckalns [49], G.I. Veres [21], M. Verweij, N. Wardle, H.K. Wöhri, A. Zagozdzinska [36], W.D. Zeuner

CERN, European Organization for Nuclear Research, Geneva, Switzerland

W. Bertl, K. Deiters, W. Erdmann, R. Horisberger, Q. Ingram, H.C. Kaestli, D. Kotlinski, U. Langenegger, T. Rohe, S.A. Wiederkehr

Paul Scherrer Institut, Villigen, Switzerland

F. Bachmair, L. Bäni, L. Bianchini, B. Casal, G. Dissertori, M. Dittmar, M. Donegà, C. Grab, C. Heidegger, D. Hits, J. Hoss, G. Kasieczka, W. Lustermann, B. Mangano, M. Marionneau, P. Martinez Ruiz del Arbol, M. Masciovecchio, M.T. Meinhard, D. Meister, F. Micheli, P. Musella, F. Nessi-Tedaldi, F. Pandolfi, J. Pata, F. Pauss, G. Perrin, L. Perrozzi, M. Quittnat, M. Rossini, M. Schönenberger, A. Starodumov [50], V.R. Tavolaro, K. Theofilatos, R. Wallny

Institute for Particle Physics, ETH Zurich, Zurich, Switzerland

T.K. Aarrestad, C. Amsler [51], L. Caminada, M.F. Canelli, A. De Cosa, C. Galloni, A. Hinzmann, T. Hreus, B. Kilminster, J. Ngadiuba, D. Pinna, G. Rauco, P. Robmann, D. Salerno, C. Seitz, Y. Yang, A. Zucchetta

Universität Zürich, Zurich, Switzerland

V. Candelise, T.H. Doan, Sh. Jain, R. Khurana, M. Konyushikhin, C.M. Kuo, W. Lin, A. Pozdnyakov, S.S. Yu

National Central University, Chung-Li, Taiwan

Arun Kumar, P. Chang, Y.H. Chang, Y. Chao, K.F. Chen, P.H. Chen, F. Fiori, W.-S. Hou, Y. Hsiung, Y.F. Liu, R.-S. Lu, M. Miñano Moya, E. Paganis, A. Psallidas, J.f. Tsai

National Taiwan University (NTU), Taipei, Taiwan

B. Asavapibhop, G. Singh, N. Srimanobhas, N. Suwonjandee

Chulalongkorn University, Faculty of Science, Department of Physics, Bangkok, Thailand

A. Adiguzel, S. Cerci [52], S. Damarseckin, Z.S. Demiroglu, C. Dozen, I. Dumanoglu, S. Girgis, G. Gokbulut, Y. Guler, I. Hos [53], E.E. Kangal [54], O. Kara, A. Kayis Topaksu, U. Kiminsu, M. Oglakci, G. Onengut [55], K. Ozdemir [56], D. Sunar Cerci [52], H. Topakli [57], S. Turkcapar, I.S. Zorbakir, C. Zorbilmez

Cukurova University, Physics Department, Science and Art Faculty, Adana, Turkey

B. Bilin, S. Bilmis, B. Isildak [58], G. Karapinar [59], M. Yalvac, M. Zeyrek

Middle East Technical University, Physics Department, Ankara, Turkey

E. Gülmez, M. Kaya [60], O. Kaya [61], E.A. Yetkin [62], T. Yetkin [63]

Bogazici University, Istanbul, Turkey

A. Cakir, K. Cankocak, S. Sen [64]

Istanbul Technical University, Istanbul, Turkey

B. Grynyov

Institute for Scintillation Materials of National Academy of Science of Ukraine, Kharkov, Ukraine

L. Levchuk, P. Sorokin

National Scientific Center, Kharkov Institute of Physics and Technology, Kharkov, Ukraine

R. Aggleton, F. Ball, L. Beck, J.J. Brooke, D. Burns, E. Clement, D. Cussans, H. Flacher, J. Goldstein, M. Grimes, G.P. Heath, H.F. Heath, J. Jacob, L. Kreczko, C. Lucas, D.M. Newbold [65], S. Paramesvaran, A. Poll, T. Sakuma, S. Seif El Nasr-storey, D. Smith, V.J. Smith

University of Bristol, Bristol, United Kingdom

K.W. Bell, A. Belyaev [66], C. Brew, R.M. Brown, L. Calligaris, D. Cieri, D.J.A. Cockerill, J.A. Coughlan, K. Harder, S. Harper, E. Olaiya, D. Petyt, C.H. Shepherd-Themistocleous, A. Thea, I.R. Tomalin, T. Williams

Rutherford Appleton Laboratory, Didcot, United Kingdom

M. Baber, R. Bainbridge, O. Buchmuller, A. Bundock, D. Burton, S. Casasso, M. Citron, D. Colling, L. Corpe, P. Dauncey, G. Davies, A. De Wit, M. Della Negra, R. Di Maria, P. Dunne, A. Elwood, D. Futyan, Y. Haddad, G. Hall, G. Iles, T. James, R. Lane, C. Laner, R. Lucas [65], L. Lyons, A.-M. Magnan, S. Malik, L. Mastrolorenzo, J. Nash, A. Nikitenko [50], J. Pela, B. Penning, M. Pesaresi, D.M. Raymond, A. Richards, A. Rose, E. Scott, C. Seez, S. Summers, A. Tapper, K. Uchida, M. Vazquez Acosta [67], T. Virdee [16], J. Wright, S.C. Zenz

Imperial College, London, United Kingdom

J.E. Cole, P.R. Hobson, A. Khan, P. Kyberd, I.D. Reid, P. Symonds, L. Teodorescu, M. Turner

Brunel University, Uxbridge, United Kingdom

A. Borzou, K. Call, J. Dittmann, K. Hatakeyama, H. Liu, N. Pastika

Baylor University, Waco, USA

R. Bartek, A. Dominguez

Catholic University of America, Washington, USA

A. Buccilli, S.I. Cooper, C. Henderson, P. Rumerio, C. West

The University of Alabama, Tuscaloosa, USA

D. Arcaro, A. Avetisyan, T. Bose, D. Gastler, D. Rankin, C. Richardson, J. Rohlf, L. Sulak, D. Zou

Boston University, Boston, USA

G. Benelli, D. Cutts, A. Garabedian, J. Hakala, U. Heintz, J.M. Hogan, O. Jesus, K.H.M. Kwok, E. Laird, G. Landsberg, Z. Mao, M. Narain, S. Piperov, S. Sagir, E. Spencer, R. Syarif

Brown University, Providence, USA

R. Breedon, D. Burns, M. Calderon De La Barca Sanchez, S. Chauhan, M. Chertok, J. Conway, R. Conway, P.T. Cox, R. Erbacher, C. Flores, G. Funk, M. Gardner, W. Ko, R. Lander, C. Mclean, M. Mulhearn, D. Pellett, J. Pilot, S. Shalhout, M. Shi, J. Smith, M. Squires, D. Stolp, K. Tos, M. Tripathi

University of California, Davis, Davis, USA

M. Bachtis, C. Bravo, R. Cousins, A. Dasgupta, A. Florent, J. Hauser, M. Ignatenko, N. Mccoll, D. Saltzberg, C. Schnaible, V. Valuev, M. Weber

University of California, Los Angeles, USA

E. Bouvier, K. Burt, R. Clare, J. Ellison, J.W. Gary, S.M.A. Ghiasi Shirazi, G. Hanson, J. Heilman, P. Jandir, E. Kennedy, F. Lacroix, O.R. Long, M. Olmedo Negrete, M.I. Paneva, A. Shrinivas, W. Si, H. Wei, S. Wimpenny, B.R. Yates

University of California, Riverside, Riverside, USA

J.G. Branson, G.B. Cerati, S. Cittolin, M. Derdzinski, R. Gerosa, A. Holzner, D. Klein, V. Krutelyov, J. Letts, I. Macneill, D. Olivito, S. Padhi, M. Pieri, M. Sani, V. Sharma, S. Simon, M. Tadel, A. Vartak, S. Wasserbaech [68], C. Welke, J. Wood, F. Würthwein, A. Yagil, G. Zevi Della Porta

University of California, San Diego, La Jolla, USA

N. Amin, R. Bhandari, J. Bradmiller-Feld, C. Campagnari, A. Dishaw, V. Dutta, M. Franco Sevilla, C. George, F. Golf, L. Gouskos, J. Gran, R. Heller, J. Incandela, S.D. Mullin, A. Ovcharova, H. Qu, J. Richman, D. Stuart, I. Suarez, J. Yoo

University of California, Santa Barbara – Department of Physics, Santa Barbara, USA

D. Anderson, J. Bendavid, A. Bornheim, J. Bunn, J. Duarte, J.M. Lawhorn, A. Mott, H.B. Newman, C. Pena, M. Spiropulu, J.R. Vlimant, S. Xie, R.Y. Zhu

California Institute of Technology, Pasadena, USA

M.B. Andrews, T. Ferguson, M. Paulini, J. Russ, M. Sun, H. Vogel, I. Vorobiev, M. Weinberg

Carnegie Mellon University, Pittsburgh, USA

J.P. Cumalat, W.T. Ford, F. Jensen, A. Johnson, M. Krohn, S. Leontsinis, T. Mulholland, K. Stenson, S.R. Wagner

University of Colorado Boulder, Boulder, USA

J. Alexander, J. Chaves, J. Chu, S. Dittmer, K. Mcdermott, N. Mirman, G. Nicolas Kaufman, J.R. Patterson, A. Rinkevicius, A. Ryd, L. Skinnari, L. Soffi, S.M. Tan, Z. Tao, J. Thom, J. Tucker, P. Wittich, M. Zientek

Cornell University, Ithaca, USA

D. Winn

Fairfield University, Fairfield, USA

S. Abdullin, M. Albrow, G. Apollinari, A. Apresyan, S. Banerjee, L.A.T. Bauerdick, A. Beretvas, J. Berryhill, P.C. Bhat, G. Bolla, K. Burkett, J.N. Butler, H.W.K. Cheung, F. Chlebana, S. Cihangir [†], M. Cremonesi, V.D. Elvira, I. Fisk, J. Freeman, E. Gottschalk, L. Gray, D. Green, S. Grünendahl, O. Gutsche, D. Hare, R.M. Harris, S. Hasegawa, J. Hirschauer, Z. Hu, B. Jayatilaka, S. Jindariani, M. Johnson, U. Joshi, B. Klima, B. Kreis, S. Lammel, J. Linacre, D. Lincoln, R. Lipton, M. Liu, T. Liu, R. Lopes De Sá, J. Lykken, K. Maeshima, N. Magini, J.M. Marraffino, S. Maruyama, D. Mason, P. McBride, P. Merkel, S. Mrenna, S. Nahn, V. O'Dell, K. Pedro, O. Prokofyev, G. Rakness, L. Ristori, E. Sexton-Kennedy, A. Soha, W.J. Spalding, L. Spiegel, S. Stoynev, J. Strait, N. Strobbe, L. Taylor, S. Tkaczyk, N.V. Tran, L. Uplegger, E.W. Vaandering, C. Vernieri, M. Verzocchi, R. Vidal, M. Wang, H.A. Weber, A. Whitbeck, Y. Wu

Fermi National Accelerator Laboratory, Batavia, USA

D. Acosta, P. Avery, P. Bortignon, D. Bourilkov, A. Brinkerhoff, A. Carnes, M. Carver, D. Curry, S. Das, R.D. Field, I.K. Furic, J. Konigsberg, A. Korytov, J.F. Low, P. Ma, K. Matchev, H. Mei, G. Mitselmakher, D. Rank, L. Shchutska, D. Sperka, L. Thomas, J. Wang, S. Wang, J. Yelton

University of Florida, Gainesville, USA

S. Linn, P. Markowitz, G. Martinez, J.L. Rodriguez

Florida International University, Miami, USA

A. Ackert, T. Adams, A. Askew, S. Bein, S. Hagopian, V. Hagopian, K.F. Johnson, T. Kolberg, H. Prosper, A. Santra, R. Yohay

Florida State University, Tallahassee, USA

M.M. Baarmand, V. Bhopatkar, S. Colafranceschi, M. Hohlmann, D. Noonan, T. Roy, F. Yumiceva

Florida Institute of Technology, Melbourne, USA

M.R. Adams, L. Apanasevich, D. Berry, R.R. Betts, I. Bucinskaite, R. Cavanaugh, O. Evdokimov, L. Gauthier, C.E. Gerber, D.J. Hofman, K. Jung, I.D. Sandoval Gonzalez, N. Varelas, H. Wang, Z. Wu, M. Zakaria, J. Zhang

University of Illinois at Chicago (UIC), Chicago, USA

B. Bilki [69], W. Clarida, K. Dilsiz, S. Durgut, R.P. Gandrajula, M. Haytmyradov, V. Khristenko, J.-P. Merlo, H. Mermerkaya [70], A. Mestvirishvili, A. Moeller, J. Nachtman, H. Ogul, Y. Onel, F. Ozok [71], A. Penzo, C. Snyder, E. Tiras, J. Wetzel, K. Yi

The University of Iowa, Iowa City, USA

B. Blumenfeld, A. Cocoros, N. Eminizer, D. Fehling, L. Feng, A.V. Gritsan, P. Maksimovic, J. Roskes, U. Sarica, M. Swartz, M. Xiao, C. You

Johns Hopkins University, Baltimore, USA

A. Al-bataineh, P. Baringer, A. Bean, S. Boren, J. Bowen, J. Castle, L. Forthomme, R.P. Kenny III, S. Khalil, A. Kropivnitskaya, D. Majumder, W. Mcbrayer, M. Murray, S. Sanders, R. Stringer, J.D. Tapia Takaki, Q. Wang

The University of Kansas, Lawrence, USA

A. Ivanov, K. Kaadze, Y. Maravin, A. Mohammadi, L.K. Saini, N. Skhirtladze, S. Toda

Kansas State University, Manhattan, USA

F. Rebassoo, D. Wright

Lawrence Livermore National Laboratory, Livermore, USA

C. Anelli, A. Baden, O. Baron, A. Belloni, B. Calvert, S.C. Eno, C. Ferraioli, J.A. Gomez, N.J. Hadley, S. Jabeen, G.Y. Jeng, R.G. Kellogg, J. Kunkle, A.C. Mignerey, F. Ricci-Tam, Y.H. Shin, A. Skuja, M.B. Tonjes, S.C. Tonwar

University of Maryland, College Park, USA

D. Abercrombie, B. Allen, A. Apyan, V. Azzolini, R. Barbieri, A. Baty, R. Bi, K. Bierwagen, S. Brandt, W. Busza, I.A. Cali, M. D'Alfonso, Z. Demiragli, G. Gomez Ceballos, M. Goncharov, D. Hsu, Y. Iiyama, G.M. Innocenti, M. Klute, D. Kovalskyi, K. Krajczar, Y.S. Lai, Y.-J. Lee, A. Levin, P.D. Luckey, B. Maier, A.C. Marini, C. Mcginn, C. Mironov, S. Narayanan, X. Niu, C. Paus, C. Roland, G. Roland, J. Salfeld-Nebgen, G.S.F. Stephans, K. Tatar, D. Velicanu, J. Wang, T.W. Wang, B. Wyslouch

Massachusetts Institute of Technology, Cambridge, USA

A.C. Benvenuti, R.M. Chatterjee, A. Evans, P. Hansen, S. Kalafut, S.C. Kao, Y. Kubota, Z. Lesko, J. Mans, S. Nourbakhsh, N. Ruckstuhl, R. Rusack, N. Tambe, J. Turkewitz

University of Minnesota, Minneapolis, USA

J.G. Acosta, S. Oliveros

University of Mississippi, Oxford, USA

E. Avdeeva, K. Bloom, D.R. Claes, C. Fangmeier, R. Gonzalez Suarez, R. Kamalieddin, I. Kravchenko, A. Malta Rodrigues, J. Monroy, J.E. Siado, G.R. Snow, B. Stieger

University of Nebraska-Lincoln, Lincoln, USA

M. Alyari, J. Dolen, A. Godshalk, C. Harrington, I. Iashvili, J. Kaisen, D. Nguyen, A. Parker, S. Rappoccio, B. Roozbahani

State University of New York at Buffalo, Buffalo, USA

G. Alverson, E. Barberis, A. Hortiangtham, A. Massironi, D.M. Morse, D. Nash, T. Orimoto, R. Teixeira De Lima, D. Trocino, R.-J. Wang, D. Wood

Northeastern University, Boston, USA

S. Bhattacharya, O. Charaf, K.A. Hahn, A. Kumar, N. Mucia, N. Odell, B. Pollack, M.H. Schmitt, K. Sung, M. Trovato, M. Velasco

Northwestern University, Evanston, USA

N. Dev, M. Hildreth, K. Hurtado Anampa, C. Jessop, D.J. Karmgard, N. Kellams, K. Lannon, N. Marinelli, F. Meng, C. Mueller, Y. Musienko [37], M. Planer, A. Reinsvold, R. Ruchti, N. Rupprecht, G. Smith, S. Taroni, M. Wayne, M. Wolf, A. Woodard

University of Notre Dame, Notre Dame, USA

J. Alimena, L. Antonelli, B. Bylsma, L.S. Durkin, S. Flowers, B. Francis, A. Hart, C. Hill, R. Hughes, W. Ji, B. Liu, W. Luo, D. Puigh, B.L. Winer, H.W. Wulsin

The Ohio State University, Columbus, USA

S. Cooperstein, O. Driga, P. Elmer, J. Hardenbrook, P. Hebda, D. Lange, J. Luo, D. Marlow, T. Medvedeva, K. Mei, I. Ojalvo, J. Olsen, C. Palmer, P. Piroué, D. Stickland, A. Svyatkovskiy, C. Tully

Princeton University, Princeton, USA

S. Malik

University of Puerto Rico, Mayaguez, USA

A. Barker, V.E. Barnes, S. Folgueras, L. Gutay, M.K. Jha, M. Jones, A.W. Jung, A. Khatiwada, D.H. Miller, N. Neumeister, J.F. Schulte, X. Shi, J. Sun, F. Wang, W. Xie

Purdue University, West Lafayette, USA

N. Parashar, J. Stupak

Purdue University Northwest, Hammond, USA

A. Adair, B. Akgun, Z. Chen, K.M. Ecklund, F.J.M. Geurts, M. Guilbaud, W. Li, B. Michlin, M. Northup, B.P. Padley, J. Roberts, J. Rorie, Z. Tu, J. Zabel

Rice University, Houston, USA

B. Betchart, A. Bodek, P. de Barbaro, R. Demina, Y.t. Duh, T. Ferbel, M. Galanti, A. Garcia-Bellido, J. Han, O. Hindrichs, A. Khukhunaishvili, K.H. Lo, P. Tan, M. Verzetti

University of Rochester, Rochester, USA

A. Agapitos, J.P. Chou, Y. Gershtein, T.A. Gómez Espinosa, E. Halkiadakis, M. Heindl, E. Hughes, S. Kaplan, R. Kunnawalkam Elayavalli, S. Kyriacou, A. Lath, K. Nash, M. Osherson, H. Saka, S. Salur, S. Schnetzer, D. Sheffield, S. Somalwar, R. Stone, S. Thomas, P. Thomassen, M. Walker

Rutgers, The State University of New Jersey, Piscataway, USA

A.G. Delannoy, M. Foerster, J. Heideman, G. Riley, K. Rose, S. Spanier, K. Thapa

University of Tennessee, Knoxville, USA

O. Bouhali [72], A. Celik, M. Dalchenko, M. De Mattia, A. Delgado, S. Dildick, R. Eusebi, J. Gilmore, T. Huang, E. Juska, T. Kamon [73], R. Mueller, Y. Pakhotin, R. Patel, A. Perloff, L. Perniè, D. Rathjens, A. Safonov, A. Tatarinov, K.A. Ulmer

Texas A&M University, College Station, USA

N. Akchurin, C. Cowden, J. Damgov, F. De Guio, C. Dragoiu, P.R. Dudero, J. Faulkner, E. Gurpinar, S. Kunori, K. Lamichhane, S.W. Lee, T. Libeiro, T. Peltola, S. Undleeb, I. Volobouev, Z. Wang

Texas Tech University, Lubbock, USA

S. Greene, A. Gurrola, R. Janjam, W. Johns, C. Maguire, A. Melo, H. Ni, P. Sheldon, S. Tuo, J. Velkovska, Q. Xu

Vanderbilt University, Nashville, USA

M.W. Arenton, P. Barria, B. Cox, J. Goodell, R. Hirosky, A. Ledovskoy, H. Li, C. Neu, T. Sinthuprasith, X. Sun, Y. Wang, E. Wolfe, F. Xia

University of Virginia, Charlottesville, USA

C. Clarke, R. Harr, P.E. Karchin, J. Sturdy

Wayne State University, Detroit, USA

D.A. Belknap, J. Buchanan, C. Caillol, S. Dasu, L. Dodd, S. Duric, B. Gomber, M. Grothe, M. Herndon, A. Hervé, P. Klabbers, A. Lanaro, A. Levine, K. Long, R. Loveless, T. Perry, G.A. Pierro, G. Polese, T. Ruggles, A. Savin, N. Smith, W.H. Smith, D. Taylor, N. Woods

University of Wisconsin – Madison, Madison, WI, USA

† Deceased.
[1] Also at Vienna University of Technology, Vienna, Austria.
[2] Also at State Key Laboratory of Nuclear Physics and Technology, Peking University, Beijing, China.
[3] Also at Institut Pluridisciplinaire Hubert Curien (IPHC), Université de Strasbourg, CNRS/IN2P3, Strasbourg, France.
[4] Also at Universidade Estadual de Campinas, Campinas, Brazil.
[5] Also at Universidade Federal de Pelotas, Pelotas, Brazil.
[6] Also at Université Libre de Bruxelles, Bruxelles, Belgium.
[7] Also at Deutsches Elektronen-Synchrotron, Hamburg, Germany.
[8] Also at Joint Institute for Nuclear Research, Dubna, Russia.
[9] Also at Suez University, Suez, Egypt.
[10] Now at British University in Egypt, Cairo, Egypt.
[11] Also at Ain Shams University, Cairo, Egypt.
[12] Now at Helwan University, Cairo, Egypt.
[13] Also at Université de Haute Alsace, Mulhouse, France.
[14] Also at Skobeltsyn Institute of Nuclear Physics, Lomonosov Moscow State University, Moscow, Russia.
[15] Also at Tbilisi State University, Tbilisi, Georgia.
[16] Also at CERN, European Organization for Nuclear Research, Geneva, Switzerland.
[17] Also at RWTH Aachen University, III. Physikalisches Institut A, Aachen, Germany.
[18] Also at University of Hamburg, Hamburg, Germany.
[19] Also at Brandenburg University of Technology, Cottbus, Germany.
[20] Also at Institute of Nuclear Research ATOMKI, Debrecen, Hungary.
[21] Also at MTA-ELTE Lendület CMS Particle and Nuclear Physics Group, Eötvös Loránd University, Budapest, Hungary.
[22] Also at Institute of Physics, University of Debrecen, Debrecen, Hungary.
[23] Also at Indian Institute of Technology Bhubaneswar, Bhubaneswar, India.
[24] Also at University of Visva-Bharati, Santiniketan, India.
[25] Also at Indian Institute of Science Education and Research, Bhopal, India.
[26] Also at Institute of Physics, Bhubaneswar, India.
[27] Also at University of Ruhuna, Matara, Sri Lanka.
[28] Also at Isfahan University of Technology, Isfahan, Iran.
[29] Also at Yazd University, Yazd, Iran.
[30] Also at Plasma Physics Research Center, Science and Research Branch, Islamic Azad University, Tehran, Iran.
[31] Also at Università degli Studi di Siena, Siena, Italy.
[32] Also at Purdue University, West Lafayette, USA.
[33] Also at International Islamic University of Malaysia, Kuala Lumpur, Malaysia.
[34] Also at Malaysian Nuclear Agency, MOSTI, Kajang, Malaysia.
[35] Also at Consejo Nacional de Ciencia y Tecnología, Mexico city, Mexico.
[36] Also at Warsaw University of Technology, Institute of Electronic Systems, Warsaw, Poland.
[37] Also at Institute for Nuclear Research, Moscow, Russia.
[38] Now at National Research Nuclear University 'Moscow Engineering Physics Institute' (MEPhI), Moscow, Russia.
[39] Also at St. Petersburg State Polytechnical University, St. Petersburg, Russia.
[40] Also at University of Florida, Gainesville, USA.
[41] Also at P.N. Lebedev Physical Institute, Moscow, Russia.

[42] Also at California Institute of Technology, Pasadena, USA.
[43] Also at Budker Institute of Nuclear Physics, Novosibirsk, Russia.
[44] Also at Faculty of Physics, University of Belgrade, Belgrade, Serbia.
[45] Also at INFN Sezione di Roma; Sapienza Università di Roma, Rome, Italy.
[46] Also at University of Belgrade, Faculty of Physics and Vinca Institute of Nuclear Sciences, Belgrade, Serbia.
[47] Also at Scuola Normale e Sezione dell'INFN, Pisa, Italy.
[48] Also at National and Kapodistrian University of Athens, Athens, Greece.
[49] Also at Riga Technical University, Riga, Latvia.
[50] Also at Institute for Theoretical and Experimental Physics, Moscow, Russia.
[51] Also at Albert Einstein Center for Fundamental Physics, Bern, Switzerland.
[52] Also at Adiyaman University, Adiyaman, Turkey.
[53] Also at Istanbul Aydin University, Istanbul, Turkey.
[54] Also at Mersin University, Mersin, Turkey.
[55] Also at Cag University, Mersin, Turkey.
[56] Also at Piri Reis University, Istanbul, Turkey.
[57] Also at Gaziosmanpasa University, Tokat, Turkey.
[58] Also at Ozyegin University, Istanbul, Turkey.
[59] Also at Izmir Institute of Technology, Izmir, Turkey.
[60] Also at Marmara University, Istanbul, Turkey.
[61] Also at Kafkas University, Kars, Turkey.
[62] Also at Istanbul Bilgi University, Istanbul, Turkey.
[63] Also at Yildiz Technical University, Istanbul, Turkey.
[64] Also at Hacettepe University, Ankara, Turkey.
[65] Also at Rutherford Appleton Laboratory, Didcot, United Kingdom.
[66] Also at School of Physics and Astronomy, University of Southampton, Southampton, United Kingdom.
[67] Also at Instituto de Astrofísica de Canarias, La Laguna, Spain.
[68] Also at Utah Valley University, Orem, USA.
[69] Also at Argonne National Laboratory, Argonne, USA.
[70] Also at Erzincan University, Erzincan, Turkey.
[71] Also at Mimar Sinan University, Istanbul, Istanbul, Turkey.
[72] Also at Texas A&M University at Qatar, Doha, Qatar.
[73] Also at Kyungpook National University, Daegu, Korea.